Report 3, 1993

GEOCHEMICAL STUDIES ON WATERS FROM THE KATWE-KIKORONGO, BURANGA AND KIBIRO GEOTHERMAL AREAS, UGANDA

Godfrey Bahati,
UNU Geothermal Training Programme,
Orkustofnun - National Energy Authority,
Grensasvegur 9,
108 Reykjavik,
ICELAND

Permanent address:
Geological Survey and Mines Department,
P.O. Box 9,
Entebbe,
UGANDA

ABSTRACT

Geochemical studies have been carried out in three geothermal areas in West and Southwest Uganda. They are the Katwe-Kikorongo, Buranga and Kibiro geothermal areas, all of which are located in the western branch of the East African Rift. For this report three geothermal and one or two cold ground water samples from each area have been analyzed and the results interpreted with the aid of speciation programmes, relational diagrams, chemical geothermometers and mixing models.

The high carbonate concentrations of the Katwe-Kikorongo and Buranga waters apparently affect their calcium and magnesium concentrations and thus throw the validity of some conventional methods of interpretation into doubt. Taking these doubts into account subsurface temperatures of at least 150-160°C have been predicted in Katwe-Kikorongo, 120-130°C in Buranga, but two sets of geothermometer temperatures have been obtained for Kibiro, 150-160°C and 200-210°C probably reflecting equilibrium states of a different age, possibly at different depths.

One of the samples from Katwe-Kikorongo was collected from an outflow on the bottom of a very saline crater lake, Lake Kitagata and is apparently mixed with a considerable amount of lake water. As this area looks a promising geothermal prospect geologically and also because the results of the chemical analysis of the sample suggested some high-temperature characteristics, it is recommended that an attempt be made to obtain a less mixed sample from the outflow and a sample of relatively pure lake water be collected to aid the interpretation of the nature of this outflow. Questions regarding the origins of the thermal water and of possible mixing patterns remain unresolved and therefore further investigations are recommended in all the three areas.

TABLE OF CONTENTS

LIST OF FIGURES

LIST OF TABLES

1. INTRODUCTION

This report is part of the training offered by the United Nations University. The Fellow attended the six months Geothermal Training Programme at the United Nations University in Iceland from April to October 1993. The programme constitutes an introductory lecture course, which provides a background knowledge on most aspects of geothermal energy resources and technology, and a specialized training in the chemistry of thermal fluids which is concluded with an extensive project report. During the training, much emphasis was put on the application of chemical geothermometers and the calculation of mixing models. Environmental aspects of thermal fluid utilization were also considered. The project comprises sample collection, analysis for major constituents and the interpretation of the analytical results. The interpretation gives insight into the role of geothermal fluid chemistry in exploration and exploitation.

One of the major applications of geochemistry in the exploration of geothermal resources involves the prediction of subsurface temperatures using chemical geothermometers. In upflow zones below hot springs and shallow drill holes, cooling of the water may occur by conduction, boiling and/or mixing with cooler water. With the aid of solute geothermometry and mixing models it is possible to evaluate temperatures in the geothermal reservoir at depth below the cooling zone, using data on chemical composition of waters from hot springs and shallow drill holes. Temperatures in geothermal reservoirs are generally not homogeneous, but variable, both horizontally and vertically. Chemical geothermometry, when applied to specific hot springs, fumaroles or shallow drillholes, can at best, be expected to reveal the temperature of the aquifer feeding the respective springs, fumaroles or drillholes. Temperatures encountered in deep drillholes may thus be higher than those indicated by chemical geothermometry of nearby springs and fumaroles, particularly if the springs and fumaroles are fed by shallow aquifers.

The Fellow used this background knowledge for estimating subsurface temperatures in the Katwe-Kikorongo, Buranga and Kibiro geothermal fields in Uganda. This should assist in identifying specific prospect areas and assigning them priorities for more detailed investigation.

2. GEOTHERMAL AREAS IN UGANDA

2.1 General description

The geothermal areas in Uganda are situated in the Western Rift which is a part of the East African Rift Valley. The Rift area stretches from the Uganda-Sudan border, down along the Uganda-Zaire border to the extreme southwestern corner of Uganda where the Mufumbiro mountains are situated. Three areas, namely Katwe-Kikorongo, Buranga and Kibiro were selected for this study (Figure 1). There are other geothermal areas to the south of Katwe-Kikorongo and to the north of Kibiro.

FIGURE 1: Map of Uganda showing the study areas

The Katwe-Kikorongo geothermal field is in one of the volcanic areas in the Western Rift of Uganda. It is located immediately to the south of the Rwenzori massif, and is bordered to the south by Lake Edward and the Kazinga Channel, which connects Lake Edward and Lake George (Figure 2). The field is characterized by a great number of apparently randomly distributed craters some of which have formed crater lakes. The area is elongated NNE-SSW, and indications of fault lines with the same direction have been found (Musisi, 1991). The eruptions have built up a pile of volcanic material, rising up to 420 m above the surrounding sedimentary terrain. The area is believed to be about 8,000 years old (Quaternary to Holocene) and the Katwe crater is believed to be one of the older ones in the field. The age has been determined by radiocarbon dating of the tuff from the mouth of river Semliki to the west. The only surface geothermal manifestations that have been found are hot springs located in the Lake Kitagata crater. The area currently serves as a tourist attraction and salt is produced by evaporation from Lake Katwe.

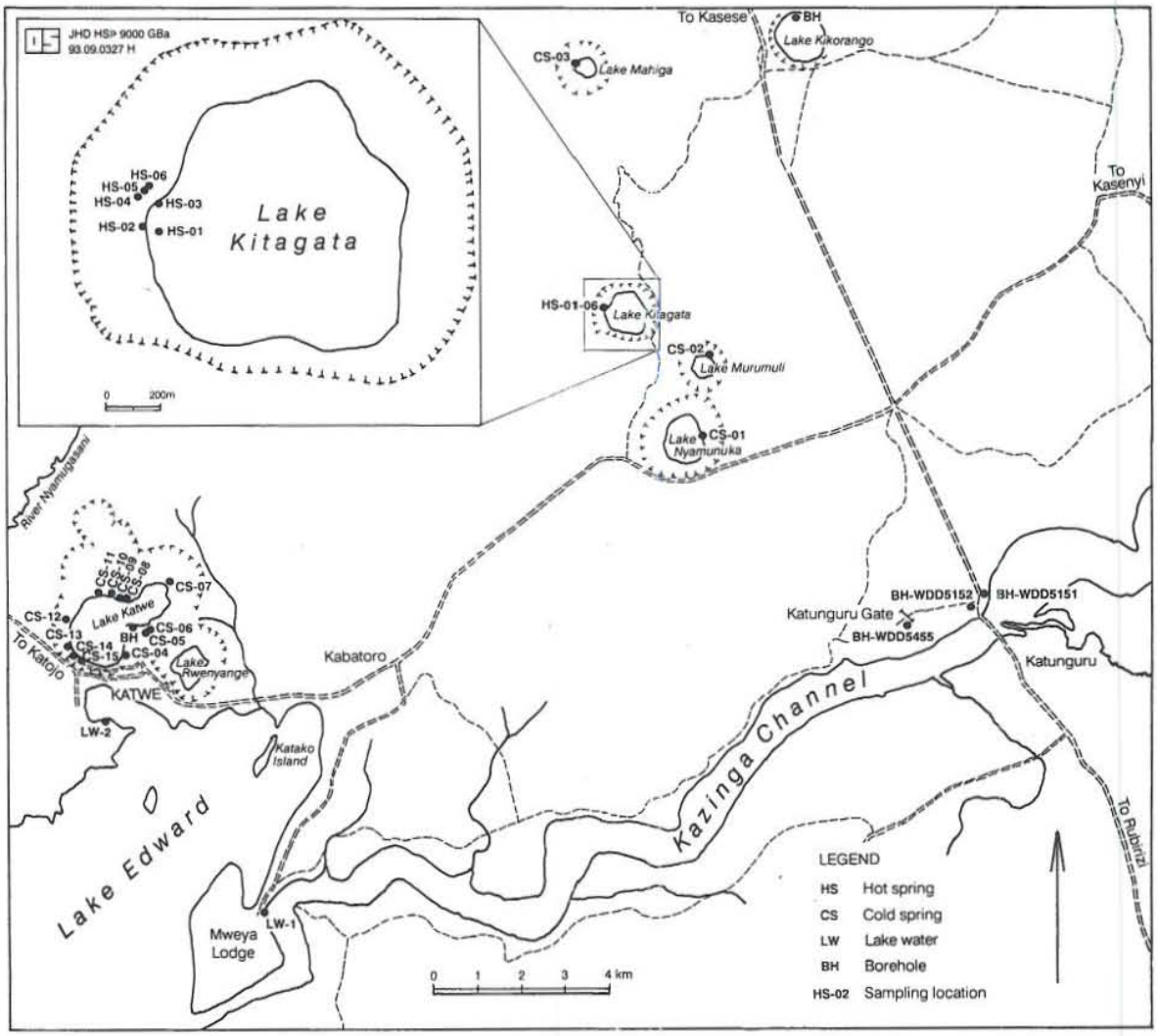

FIGURE 2: Map of the Katwe-Kikorongo geothermal area with sampling sites

The Buranga (Sempaya) geothermal area is located in Kasitu sub-county, Bwamba county of Bundibugyo district, 50 km off the Fort Portal-Bundibugyo road (Figure 3). The field is located at the periphery of the Semliki forest, near the base of the Bwamba escarpment which fronts northwest Rwenzori Mountain. The surface manifestations in this area are hot springs which are close to boiling. The hot springs emerge at the surface through Epi-Kaiso beds and "Peneplain Gravel" sediments. The sands and clays are known as Kaiso-Kisegi beds. They overlie pre-

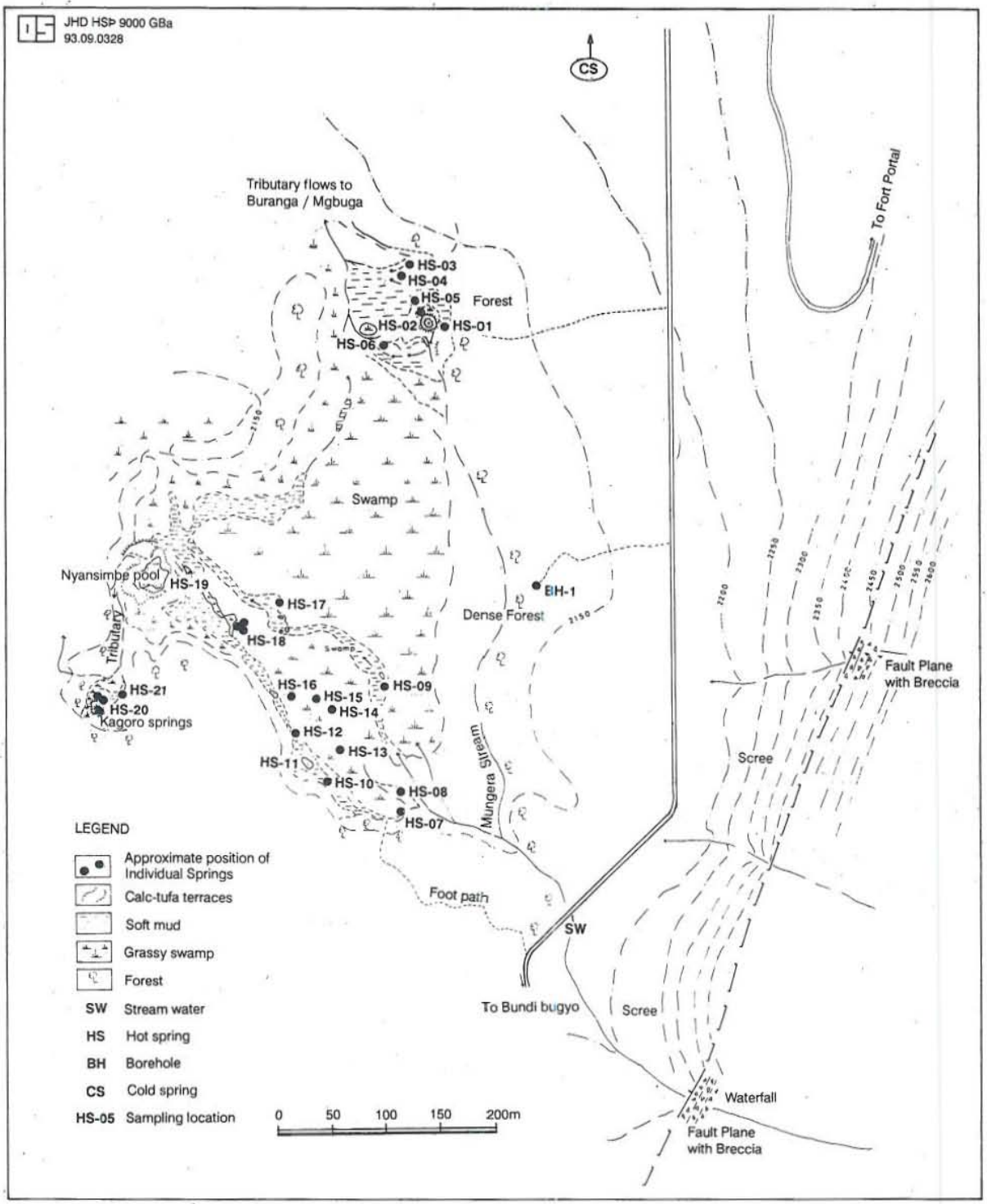

FIGURE 3: Map of the Buranga geothermal area with sampling sites

Cambrian migmatites and gneisses. All the main springs have deposited carbonates, and silica deposits can be seen lining one of the orifices at Mumbuga. The hot springs currently serve as tourist attractions and as bathing places for the local population.

The Kibiro geothermal area is situated on the eastern shore of Lake Albert (Figure 4). It lies on a narrow stony plain of about ¾ km in width between the lake shore and the foot of the

approximately 300 m high escarpment that forms the eastern margin of the Rift valley of Uganda. The altitude of Lake Albert is 610 m a.s.l. The surface manifestations in this area are hot springs. They are located within the Lake depression which contains a considerable thickness of Tertiary to Holocene deposits consisting of Kaiso beds underlain by older Kisegi beds. The main springs emerge from the rubble of fault breccia. Both the hot springs and streams in this area have deposited pyrrhotite and sulphur. The hot springs are currently being used as a source of salt production which has been going on in the area for at least nine centuries (Connah et al., 1990).

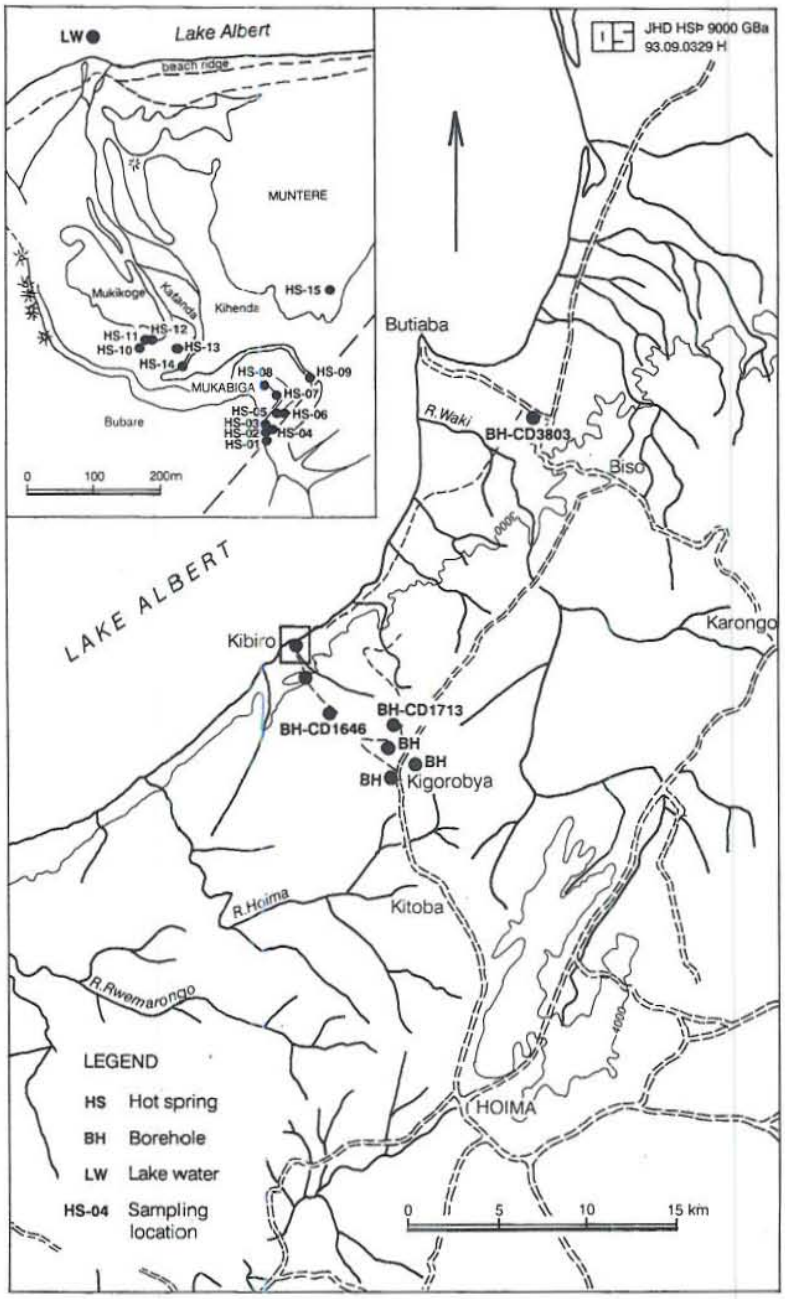

FIGURE 4: Map of the Kibiro geothermal area with sampling sites

2.2 Previous studies

The Katwe-Kikorongo geothermal area

Stanley (1890), was the first to describe the salt works of Lake Katwe, and he measured the temperatures of 29.1°C and 32°C for the lake and one spring respectively, although he failed to recognize the origins of the craters. Scott-Elliot (Scott-Elliot and Gregory, 1895), identified the three volcanic fields south and east of Rwenzori Mountains. These are Fort Portal, Katwe-Kikorongo and Bunyaruguru.

Wayland (1935) listed 45 hot and/or mineralized springs in Uganda. One spring is listed at lake Katwe on a small tufa in the lake. Its temperature is slightly higher than that of the lake water. Wayland points out that in Uganda thermal waters are found in Pre-Cambrian and Tertiary age rocks and that hot springs tend to occur in areas associated with earth movements. Detailed chemical analyses were carried out on samples from various hot springs in Uganda by Dixon and Morton (1967, 1970) in whose report the thermal springs of Lake Kitagata are first mentioned. Arad and Morton (1969), presented a number of water analyses from various springs in Uganda.

They discuss the origins of mineral springs and conclude that their source is juvenile, although the water may be meteoric. Sharma (1971), described one thermal spring at Lake Kitagata and interpreted the chemical results obtained earlier. Its temperature was 58°C, a flow rate estimated at 0.4 l/s, and the Na/K atomic ratio of this saline spring was interpreted to indicate a subsurface temperature of 230°C.

TABLE 1: Katwe-Kikorongo, crater lakes

Location	Elevation (m a.s.l.)	Temperat. (°C)	Conduct. (μS)
L. Kitagata	910	32.5	132000
L. Katwe	880	26.0	173300
L. Murumuli	890	29.5	65800
L. Mahiga	908	35.1	113600
L. Nyamunuka	885	25.3	81400
L. Rwenyange	820	32.0	32700
L. Kikorongo	900	30.1	24800
L. Edward	910	26.7	202

Gislason et al. (1993), described the surface manifestations of the Katwe-Kikorongo volcanic field and carried out temperature, flow rate and conductivity measurements on the waters of the crater lakes. The results are shown in Table 1. Warm springs were only located in the Lake Kitagata crater. Several springs were located on the western side of the lake (Figure 2). The results of the measurements on the warm springs of Lake Kitagata are summarized in the Table 2.

TABLE 2: Katwe-Kikorongo, Lake Kitagata hot springs

Location	Spring no.	Temp. (°C)	Cond. (μS)	Flow (l/s)
L. Kitagata	HS-01	65.0	139000	
L. Kitagata	HS-02	56.6	21500	>0.024
L. Kitagata	HS-03	64.3		
L. Kitagata	HS-04	65.8		0.052
L. Kitagata	HS-05	66.6	25500	0.031
L. Kitagata	HS-06	67.3		0.031

The Buranga (Sempaya) geothermal area

Wayland (1935) noted that the distribution of the hot springs is closely related to faulting. This was noted to be a regional trend and also characteristic of Buranga. In all, Wayland described 14 hot mineral springs, 11 cold mineral springs and 5 non-mineral hot springs in Uganda, the one he described in Buranga being a hot sulphurous spring. No chemical analysis was done. Arad and Morton (1969), described the geological setting and chemistry of mineral springs and saline lakes in western Uganda. The Buranga hot springs were described, including the physical characteristics, and samples of the fluid were subjected to chemical analysis. Sharma (1970), continued the search for the possible occurrence and use of geothermal energy in Uganda. Using previous data, he reviewed the possibilities and recommended preliminary investigations. In 1971, he carried out a survey to initiate the "Geothermal development programme". In his survey; he

described a number of thermal springs, measured their temperatures, and determined their flow rates and pH. He also collected water samples for chemical analysis and published the results (Sharma, 1971). Later, Sharma (1973), interpreted the chemical results for thermal waters of Lake Kitagata, Buranga, Kibiro and a few other areas. The chemical analyses had been done in 1972 by Pollock in the GSMD assay laboratory in Entebbe, and Glover in the Olkaria laboratory, Kenya. In his report interpretations were made by comparing results for silica concentrations and Na/K atomic ratios.

Stefansson (1987) published the results of Glover and Pollock after treating the data using modern methods. He used the "WATCH" programme to compute the aqueous speciation at depth from which he calculated the quartz and Na/K geothermometer temperatures using the temperature functions of Fournier (1977) and Arnorsson et al. (1983b) respectively.

Maasha-Ntungwa (1974), carried out electrical resistivity and micro-earthquake surveys along two short profiles in Buranga and his results are summarized as follows:

i) The shallow (<250 m) vertical electrical soundings at Buranga indicated low resistivity which was attributed to thermal fluids at approximately 160°C. Higher temperatures could occur at greater depths.

(ii) The Buranga field was not associated with any micro-earthquakes although the neighbouring areas showed high seismic activity. Lack of micro-earthquakes in itself, is not conclusive, although it is suggestive of a liquid dominated system.

(iii) The source of hot water is situated west of Mumbuga at a depth of 250 m or more.

Gislason et al. (1993), described the surface manifestations of the Buranga geothermal area and carried out temperature, flow rate and conductivity measurements. The results are shown in Table 3. The Buranga geothermal area can be divided into three main groups of hot springs, namely Mumbuga, Nyansimbe and Kagoro. They are situated on a line roughly parallel to the fault scarp about 0.5 km to the east (Figure 3).

The Kibiro geothermal area

Gislason et al. (1993), described the surface manifestations in this area and carried out temperature, flow rate and conductivity measurements. The main hot springs are located in an area known as Mukabiga. They emerge from a rubble of fault breccia and are located on a fault. Other minor hot springs are located in an excavated, low ground area about 200 m to the northwest (Figure 4). The temperature range around the Mukabiga set, which comprises nine hot springs is 57-84°C and the conductivity range 7620-7880 μS, while that of the other group is 33-71.1°C with the conductivity in the range of 7600-8400 μS. The flow rate was determined to be 4 l/s for Mukabiga and 2.5 l/s for the others and hence the total flow rate for the hot springs is 6.5 l/s. Further north of Mukabiga, is an area known as Muntere with a few seepages. The temperature range in this area is 33-45°C and the conductivity is in the range of 7760-9120 μS, which is a little higher than in the other two areas.

TABLE 3: Buranga hot springs

Location	No.	Temp. (°C)	Conduct. (μS)	Flow (l/s)
Mumbuga	HS-02	93.4	19400	6.5
Mumbuga	HS-03	85.5	19880	
Mumbuga	HS-04	93.3	19050	
Mumbuga	HS-05	93.6	18000	
Mumbuga	HS-06			
Nyansimbe	HS-07			0.1
Nyansimbe	HS-08	60.4	22300	0.3
Nyansimbe	HS-09	96.4	20300	
Nyansimbe	HS-10			0.5
Nyansimbe	HS-11			
Nyansimbe	HS-12			
Nyansimbe	HS-13	80.3	22600	0.5
Nyansimbe	HS-14			
Nyansimbe	HS-15			
Nyansimbe	HS-16			
Nyansimbe	HS-17	98.3	19500	1.5
Nyansimbe	HS-18			
Nyansimbe	HS-19	85.8	19900	10
Kagoro	HS-20	89.0	18000	3
Kagoro	HS-21	90.6	22700	

3. SAMPLING AND CHEMICAL ANALYSIS

3.1 Sampling

"The credibility and usefulness of geochemical data depends on the methods used and the care taken in the collection of samples. For this reason it is recommended that geochemists undertake the fieldwork. If the sampling conditions are not well known, the significance of analytical results may not be fully appreciated. A person without a chemical knowledge may contaminate samples during collection, or volatile constituents may be lost from samples by faulty handling. It is also unrealistic to expect a geochemist to take a detailed interest in an area with which he has no practical association" (Ellis and Mahon, 1977, p. 163).

The above quotation is an appropriate reminder to those using geochemical methods to explore geothermal areas. In the field it is important to keep a complete record of samples collected and a description of sample locations. A convenient field record card is recommended and an outline of such a card is shown in Appendix I.

A funnel connected to rubber tubing was submerged into the water. The tubing was fitted to a cooling coil of stainless steel placed in a bucket of cold water. The water from the spring was made to flow through the tubing and the cooling coil, making sure that the far end of the coil was at a lower level than the water level in the spring so that gravity flow could be established if possible. Where this was not possible a hand pump was used to pump the water through. When the sampling apparatus had been set up and the water cooled to ambient temperature, the samples were collected. The general set-up and the apparatus used for the collection of geothermal water is shown in Appendix I. First the pump and filter flask were directly connected to the cooling coil and 100 ml of sample collected. A small amount of this was poured into a beaker and pH, conductivity and temperature measured. Three 10 ml portions of sample were placed in 100 ml volumetric flasks and filled to the mark with distilled water. The bottles were labelled Rd for SiO_2. Secondly the filtering apparatus with a 0.2 micrometre filter was connected to the cooling coil and 700 ml of sample collected. A 100 ml portion of this sample was put in a sampling bottle, 1 ml of conc. HCl added and labelled Fa. Another 100 ml portion of the filtered sample was put in a similar bottle, 2 ml of 0.2M Zinc acetate added and labelled Fp. Lastly a 500 ml portion of the original sample was transferred to a plastic bottle and labelled Fu. Summary of the sample fractions collected is presented in Appendix I. The locations of sampling sites for the Katwe-Kikorongo, Buranga and Kibiro geothermal fields are shown in Figures 2, 3 and 4 respectively.

3.2 Analysis and results

Analysis of the water samples for pH, conductivity, total carbonate and hydrogen sulphide was performed in the field and the rest of the constituents in the Orkustofnun geochemical laboratory. The analytical methods used are listed in Table 4.

The analytical results are presented in Table 5. Samples number 005, 015, 025 and 026 are non-thermal, while the rest are geothermal samples.

TABLE 4: Analytical methods

Constituent	Sample fraction	Method	Detection limit (mg/l)
pH	Ru	pH-meter with a glass electrode	-
Total sulphide as H_2S_2S	Ru	Titration with 0.001M mercuric acetate and dithizone as indicator	0.04
Total carbonate as CO_2	Ru	Titration with 0.1N HCl using a pH-meter	1.0
Conductivity	Ru	Conductivity meter	-
Total dissolved solids	Fu	Gravimetric after drying at 180-260°C	2.5
Sodium (Na)	Fa	Atomic absorption spectrophotometry	0.001
Potassium (K)	Fa	Atomic absorption spectrophotometry	0.001
Calcium (Ca)	Fa	Atomic absorption spectrophotometry	0.001
Magnesium (Mg)	Fa	Atomic absorption spectrophotometry	0.001
Silica (SiO_2)	Ru/Rd	Spectrophotometric as (yellow) silicomolybdate complex	0.5
Iron (Fe)	Fa	Atomic absorption spectrophotometry in a graphite furnace	0.0001
Aluminium (Al)	Fa	Atomic absorption spectrophotometry in a graphite furnace	0.001
Chloride (Cl)	Fu	Ion chromatography	0.025
Sulphate (SO_4)	Fp	Ion chromatography	0.020
Fluoride (F)	Fu	Selective electrode with a pH mV-meter	-
Boron (B)	Fu	Spectrophotometric after complexation with azomethine-H	0.005

NB: Ru - raw, untreated water sample
Fa - filtered, acidified water sample
Fp - filtered, precipitated water sample
Fu - filtered, untreated water sample
Rd - raw, diluted water sample

TABLE 5: Analytical results (in mg/kg)

Area	Location no.	Sample no.	Temp. (°C)	pH/°C	CO_2	H_2S	SiO_2	B	Na	K	Mg	Ca	F	Cl	SO_4	Al	Fe	Li	TDS
Katwe-	KTKAHS-05	006	66.6	8.41/26	3105	<0.1	88.5	0.91	9310	644	0.85	0.60	39.56	2430	13420	0.010	0.02	0.06	27770
Kikorongo	KTKAHS-02	007	56.6	8.03/26	2544	<0.1	102.4	0.64	6510	523	6.27	1.45	24.30	1770	8965	0.016	0.01	0.03	19410
	KTKNLW-01	018	61.2	9.57/24	17785	40.66	369.0	6.45	84200	4740	0.74	0.90	385.7	20800	108900	0.073	0.02	0.07	244100
	KTWDD5455	005	26.6	6.95/27.5	1000	<0.1	48.0	0.06	952	89.7	232	296	0.577	723	1800	0.020	0.04	0.02	4870
Buranga	BRMUHS-05	010	93.6	7.73/20	2411	<0.05	74.5	4.26	5160	190	2.27	2.56	25.08	3490	3575	0.014	0.05	1.30	14030
	BRNSHS-20	012	89.0	7.50/22	2798	0.26	109.3	4.83	5950	219	2.19	2.69	27.78	4030	4155	0.019	0.02	1.47	16400
	BRNSHS-17	014	98.2	8.57/21	2635	<0.05	78.8	5.13	6270	235	0.28	0.39	29.58	4200	4400	0.540	0.39	1.51	17080
	BRNSHSW	015	21.8	7.52/20	57	n.d	36.0	0.03	11.1	3.73	3.61	11.2	0.161	1.76	1.75	0.011	0.02	0.008	74
Kibiro	KBMBHS-02	019	86.5	7.06/24	146	10.37	111.6	2.31	1530	169	8.14	62.0	4.703	2490	47.1	0.037	<0.01	1.50	4576
	KBKNHS-14	021	71.8	7.14/25	155	17.31	113.3	2.28	1480	165	9.21	65.7	4.486	2450	16.7	0.044	<0.01	1.46	4384
	KBMEHS-15	022	39.5	8.05/25	115	<0.04	135.5	2.47	1570	182	8.71	75.9	4.910	2590	51.4	0.029	0.03	1.53	4548
	KBCD1713	025	23.6	6.26/22	130	n.d.	68.4	0.27	12.4	2.64	8.03	14.8	0.120	5.18	5.25	0.007	0.74	0.003	124
	KBCD1646	026	24.9	6.72/22	232	n.d.	77.6	0.05	50.6	7.50	39.5	138	0.145	123	227	0.014	0.72	0.02	680

n.d. = not determined

4. THE CHEMISTRY OF THE FLUIDS

4.1 Hydrothermal alteration

Studies on hydrothermal alteration-mineralogy and well fluid composition in geothermal fields worldwide have demonstrated that a chemical equilibrium between all dissolved constituents, except chloride, and alteration minerals is closely reached (Giggenbach, 1988; Arnorsson et al., 1978, 1983a). It is the result of these studies that aids the groundwork for the basic assumption in chemical geothermometry that a mineral/solute equilibrium exists in the reservoir. In contrast to the hot waters, surface waters, non-thermal ground waters and lukewarm spring waters do not attain overall equilibrium with weathering or hydrothermal minerals. Equilibrium between some aqueous constituents and some alteration minerals may be closely reached, or the water-rock system may be far from reaching equilibrium. The fluids sampled are likely to have reached some complex steady-state composition reflecting the combined effects of initial fluid composition, the kinetics of primary mineral dissolution and secondary mineral deposition at changing temperatures, in addition to vapour loss, dilution and mixing with fluids of different origin (Giggenbach, 1984).

Hydrothermal alteration by geothermal waters is essentially hydrogen ion metasomatism (Giggenbach, 1981). It involves the absorption of protons by the rock and a simultaneous release of other cations (Gislason and Eugster, 1987a; b) as well as dissolution of silica and soluble salts which are present in low concentrations in common rocks. During the alteration process, the primary rock constituents dissolve and secondary (hydrothermal) minerals precipitate. The constituents dissolved in the water tend to equilibrate with the precipitating hydrothermal minerals. They represent stable and meta-stable phases in the system, whereas the primary rock minerals are generally unstable. For most waters dissolved carbon dioxide and aqueous silica (H_4SiO_4) represent the main proton donors which condition the dissolution of primary rock constituents. In some systems hydrogen sulphide may also be important. The dissolved silica is derived from the altered rock. The hydrogen sulphide may also be derived from the rock or from a magmatic source (Gunnlaugsson, 1977). The carbonate may be derived from several sources: atmospheric, organic, the dissolution of the rock, metamorphic reactions and magma intrusions. Dissolved silica is only an important proton donor, at a high pH (above about 9) at which a significant fraction of the dissolved silica ionizes and, thus, generates protons.

To maintain the water close to equilibrium with the precipitating secondary minerals, the rate of precipitation must be such that it is able to cope with the transfer of the mass from the dissolving primary rock constituents to the solution. Waters with a large source of protons, such as carbon dioxide waters, must react more forcibly with their host rock than waters with a limited source in order to reach equilibrium with secondary minerals. Thus, there is a greater probability that "proton rich waters" significantly depart from equilibrium with secondary minerals than "proton poor waters". Consequently, there is less probability that chemical geothermometers apply to "proton rich waters" than to "proton poor waters", other things being constant.

4.2 Equilibrium calculations

The complex reactions that take place in hydrothermal systems are handled by speciation programmes, such as the WATCH programme which was used for this study (Arnorsson et al., 1982; Arnorsson and Bjarnason, 1993). The programme handles three main models for geothermal fluids. The first of these is applicable to wet-steam wells with "excess enthalpy", i.e. where liquid water and steam coexist in the reservoir. The second model is appropriate for hot-water wells and hot spring fluids that have not boiled before sample collection, and wet steam

wells in single-phase (liquid) aquifers. The third model describes boiling hot springs where steam and gas have been lost prior to sampling by boiling of the fluid from the reference temperature down to the assumed final temperature. Here, the original composition is reconstructed by computing and adding back the lost steam and gas. The input to the programme is from a file containing a component analysis of each phase of the geothermal fluid at the surface, including the water pH and the temperature at which it was measured. Other input, which is provided interactively from the terminal, includes a value for the reference temperature, that is the temperature at which the composition is to be calculated. The reference temperature can be chosen as the measured temperature of the well or spring, or as any arbitrary temperature, a chalcedony, quartz, or sodium-potassium chemical geothermometer temperature. The programme reads data from the input file and computes the chemical composition of the deep water, activities of species, redox potentials, partial pressures of gases, ionic balance, ion activity products and solubility products of selected minerals and prints the results in the output file. A printout of a sample output file is displayed in Appendix II.

The concentrations of the aqueous species considered in the programme are expressed in terms of the component concentrations by mass balance equations, and the chemical equilibria between the species are expressed as mass action equations. The two sets of equations are solved simultaneously by an iterative procedure. This procedure is carried out a few times during each run of the programme. The programme contains provisions for 67 different species, in addition to H^+ and OH^- which are treated separately.

4.3 Triangular diagrams

Simple procedures have been described allowing an initial assessment of the geothermal potential of an area to be made by extracting much of the information carried by a given constituent in a comparatively straight-forward manner (Giggenbach 1988). The procedures frequently require an initial, assessment of correlations among sets of various constituents, a task commonly carried out by the use of triangular diagrams. Giggenbach (1988) has pioneered techniques for the derivation of Na-K-Mg-Ca geoindicators. Considering Na, K and Mg as an example, a triangular diagram (Figure 5) can be used to distinguish between equilibrated waters, partially equilibrated (including mixed) waters and immature waters. This helps weeding out waters not suitable for the application of solute geothermometers. At the same time it allows the degree of deeper re-equilibration and mixing of waters of different origins to be assessed for a large number of samples. The simultaneous evaluation also facilitates the delineation of trends and groupings among water discharges and, from these, of variations in the nature and intensity of processes affecting the rising waters. The construction of the diagram is essentially based on the temperature dependence of the two reactions:

$$K\text{-}feldspar + Na^+ = Na\text{-}feldspar + K^+ \qquad (1)$$

and

$$2.8\,K\text{-}feldspar + 1.6\,water + Mg^{2+} = 0.8\,K\text{-}mica + 0.2\,chlorite + 5.4\,silica + 2\,K^+ \qquad (2)$$

They both involve minerals of the full equilibrium assemblage after isochemical recrystallization of an average crustal rock under conditions of geothermal interest. Na, K and Mg concentrations of waters in equilibrium with this assemblage are accessible to rigorous evaluation. The theoretical temperature dependence of the corresponding concentration quotients then may be used to derive two geothermometers:

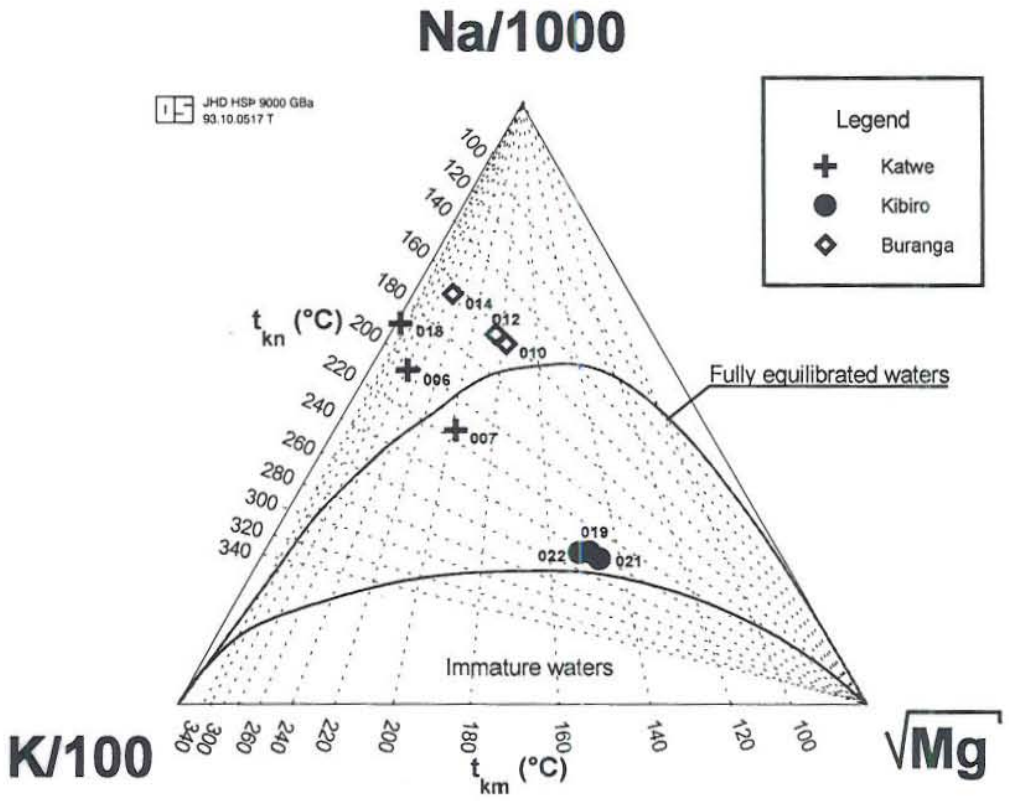

FIGURE 5: Na-K-Mg triangular diagram for evaluation of equilibrium states of geothermal waters from Katwe-Kikorongo, Buranga and Kibiro

$$t_{kn} = \frac{1390}{(1.75 - L_{kn})} - 273 \qquad (3)$$

and

$$t_{km} = \frac{4410}{(14.0 - L_{km})} - 273 \qquad (4)$$

where

$$L_{kn} = \log(\frac{C_K}{C_{Na}}), \quad L_{km} = \log(\frac{C_K^2}{C_{Mg}}) \quad and \quad C_i \ in \ mg/kg$$

Individual application of Equations 3 and 4 frequently leads to significantly different apparent temperatures of equilibration. This observation is readily explained in terms of differing rates of re-adjustment of the two reactions to changes in the physical environment encountered by the rising waters. Reaction 4 was found to respond much faster and, therefore, gives usually lower temperature estimates. The values of L_{km} are also very sensitive to the admixture of non-equilibrium acid waters, while L_{kn} is much less affected by such shallow processes. By combining the two sub-systems, a method is obtained allowing the degree of attainment of water-rock equilibrium to be assessed and unsuitable samples to be eliminated. The coordinates of a point on the diagram are calculated according to the following equations:

$$S = \frac{C_{Na}}{1000} + \frac{C_K}{100} + \sqrt{C_{Mg}} \quad (5)$$

$$\%\text{-}Na = \frac{C_{Na}}{10S} \quad (6)$$

$$\%\text{-}Mg = 100\frac{\sqrt{C_{Mg}}}{S} \quad (7)$$

Because of the non-linear term C_K^2, the square root is taken of the Mg concentrations. Sodium and potassium concentrations are divided by 1000 and 100 respectively in order to accommodate most geothermal waters. The data points for Katwe-Kikorongo and Buranga plot close to the full equilibrium line but the magnesium concentration may be low due to the high carbonate concentrations of these waters and hence the shifting of most of the points beyond the equilibrium curve. The data points from Kibiro plot in the area of partially equilibrated (including mixed) waters. This is probably due to mixing of the thermal fluid with cold ground or meteoric water as it moves to the surface. The Na/K and K/Mg geothermometer temperatures derived from this diagram are presented in Table 6.

TABLE 6: Equilibrium temperatures predicted from the Na-K-Mg diagram (Giggenbach 1988)

Area	Na/K temperature (°C)	K/Mg temperature (°C)
Katwe-Kikorongo	200-220	200-260
Buranga	160-170	180-240
Kibiro	240	150

The Na/K geothermometer of Giggenbach (1988) gives higher results than most other geothermometers. The K/Mg geothermometer gives high results for Katwe-Kikorongo and Buranga areas probably due to loss of magnesium in the upflow zone and low results for Kibiro area probably due to mixing with cold water and the attendant gain of magnesium. Generally, geothermometry temperatures derived directly from this diagram tend to be very high because it uses the analytical concentrations and not the activities which should be used for waters of high salinity.

Figure 6 shows a triangular diagram based on the relative concentrations of the three major anions i.e. Cl, SO_4 and HCO_3. Its use is based on the assumption that most ionic solute geothermometers "work" only if used with close to neutral waters containing chloride as a major anion. The position of a data point in such a diagram is simply obtained by first forming the sums of the concentrations C_i in (mg/kg) of all the three constituents involved. In this case

$$S = C_{Cl} + C_{SO_4} + C_{HCO_3} \quad (8)$$

The next step consists of the evaluation of %-Cl and %-HCO_3 according to

$$\%-Cl = \frac{100\,C_{Cl}}{S} \tag{9}$$

and

$$\%-HCO_3 = \frac{100\,C_{HCO_3}}{S} \tag{10}$$

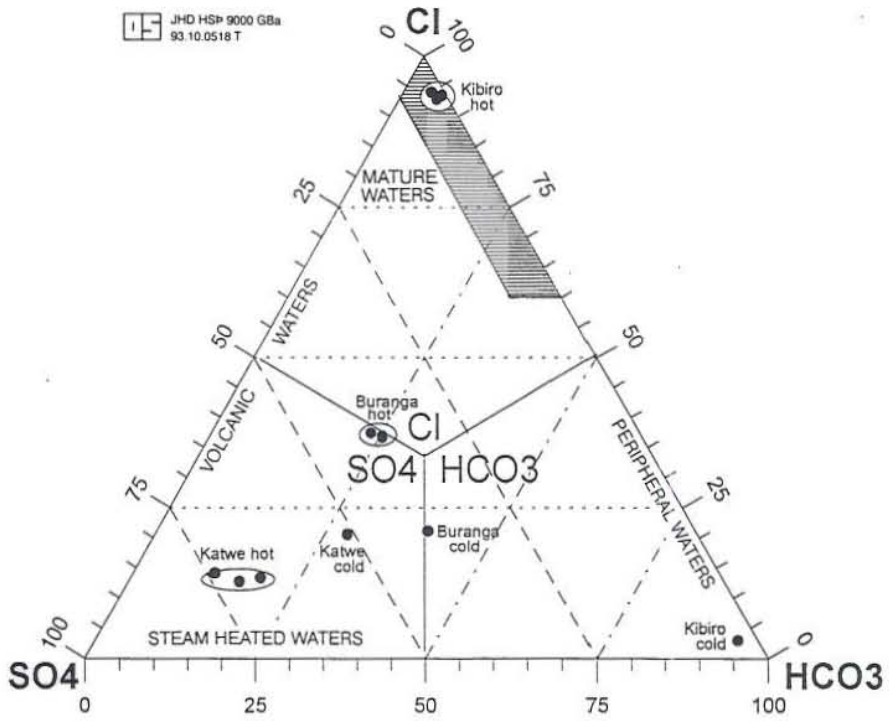

FIGURE 6: Relative Cl, SO_4 and HCO_3 concentrations of thermal and non-thermal waters of the Katwe-Kikorongo, Buranga and Kibiro areas on weight basis (mg/kg)

The compositional ranges are indicated for several typical groups of thermal waters such as volcanic and steam heated waters formed by the absorption of high temperature, HCl-containing volcanic, or lower temperature, H_2S-containing "geothermal" vapours, into ground water. Most geochemical techniques are not suitable for application to these generally quite acid waters. The most suitable group comprises neutral, low sulphate, high chloride "geothermal" waters along the Cl-HCO_3 axis, close to the chloride corner (shaded area). With neutral, but high bicarbonate waters, considerable caution is required in the application of most "geoindicators".

Figure 6 not only allows the weeding out of unsuitable waters, but may also provide an initial indication of mixing relationships, with e.g. chloride waters forming a central core grading into HCO_3 waters towards the margins of a thermal area. High sulphate steam-heated waters are usually encountered over the more elevated parts of a field. The degree of separation between data points for high chloride and bicarbonate waters gives an idea of the relative degrees of interaction of the carbon dioxide charged fluids at lower temperatures, and the HCO_3 concentration increasing with time and distance travelled underground. The data points for the Kibiro geothermal area plot close to the chloride corner and this suggests that these waters are chloride-mature, while the waters of Katwe-Kikorongo geothermal area are sulphate, volcanic and steam heated. The Buranga waters are chloride to sulphate waters.

4.4 Solute geothermometers

The calculation of geothermal reservoir temperatures with the aid of chemical geothermometers, using the data on chemical composition of springs, fumaroles and shallow drillholes, involves various assumptions and simplifications. The basic assumption is that a temperature-dependent equilibrium is attained in the geothermal reservoir between solute(s)/gas(es) and mineral(s). Some gas geothermometers are based on assumptions about specific gas-gas equilibria. Further, it is assumed that the respective solute or gas concentrations are not affected by chemical reactions in the upflow zone where cooling occurs. Several geothermometers have been calibrated to predict reservoir temperatures in geothermal systems (e.g. Fournier and Potter, 1982; Fournier, 1977; Arnorsson et al., 1983b).

Table 7 shows geothermometry results for the Katwe-Kikorongo, Buranga and Kibiro geothermal areas. In Western Uganda, the basement rock formation is of pre-Cambrian age and the most important silica mineral in them and the overlying sediments is quartz. Therefore, it was assumed that quartz is the mineral controlling the silica concentration of the geothermal fluid and thus the quartz geothermometer was applied instead of the chalcedony one. The cation geothermometers used are based on the activities as calculated by the WATCH programme and not on the concentrations of the cations because of the high salinity of the waters. The quartz and K/Mg geothermometer give lower results than the Na/K geothermometer, probably due to quick re-equilibration as the fluid cools in the upflow zone. The K/Mg geothermometer gives higher results than the Na/K geothermometer for Katwe-Kikorongo and Buranga areas, probably due to loss of magnesium as magnesium carbonate because of the high carbonate content of the waters.

TABLE 7: Geothermometry results, temperatures in °C

Area	Sample no.	Meas.	Quartz (1)	Na/K (2)	H_2S (3)	H_2CO_3 (4)	CaH (5)	K/Mg (6)
Katwe-Kikorongo	006	66.6	105	142	-	-	160	>250
	007	56.6	122	157	-	-	161	250
Buranga	010	93.6	113	102	-	-	161	225
	012	89.0	132	100	146	-	175	226
	014	98.2	100	103	-	-	158	>250
Kibiro	019	86.5	142	212	213	198	142	160
	021	71.8	142	213	221	200	136	156
	022	39.5	156	217	-	196	117	164

(1) Fournier and Potter (1982), WATCH programme
(2) Arnorsson et al. (1983b), WATCH programme
(3), (4), (5) and (6) temperature functions presented in Table 5 of Arnorsson et al. (1983b).

The CaH geothermometer results can be explained in the same way as for the K/Mg geothermometer since the concentrations of magnesium and calcium are controlled by the same factors. There is a good agreement between Na/K, H_2S and H_2CO_3 geothermometers for the Kibiro waters.

The H_2CO_3 geothermometer could not be applied to the Katwe-Kikorongo and Buranga areas because of the high carbonate concentration which is not likely to be in equilibrium with the

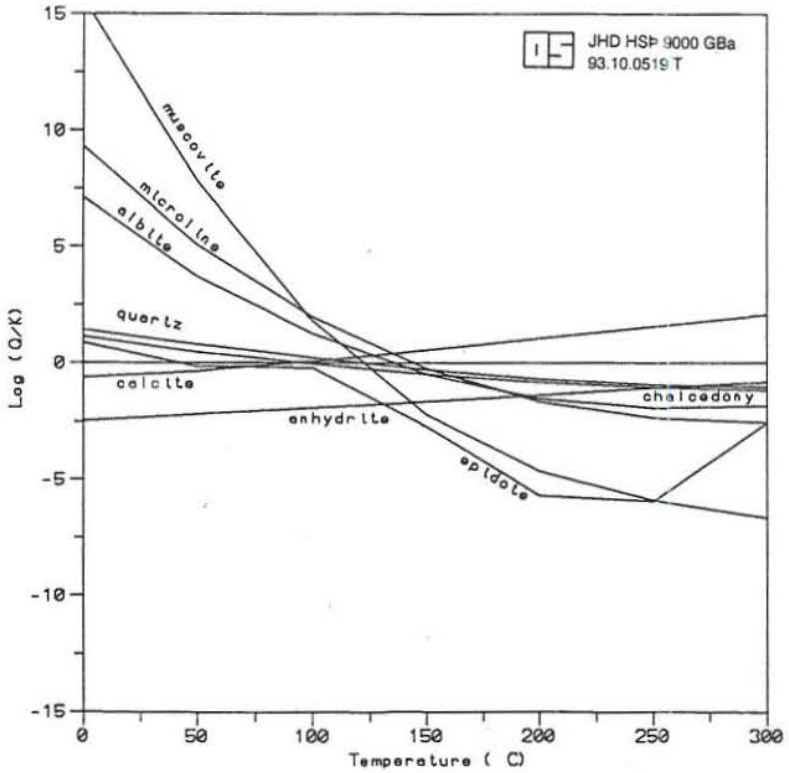

FIGURE 7: The saturation state of some minerals in water from the Katwe-Kikorongo area, sample No. 007

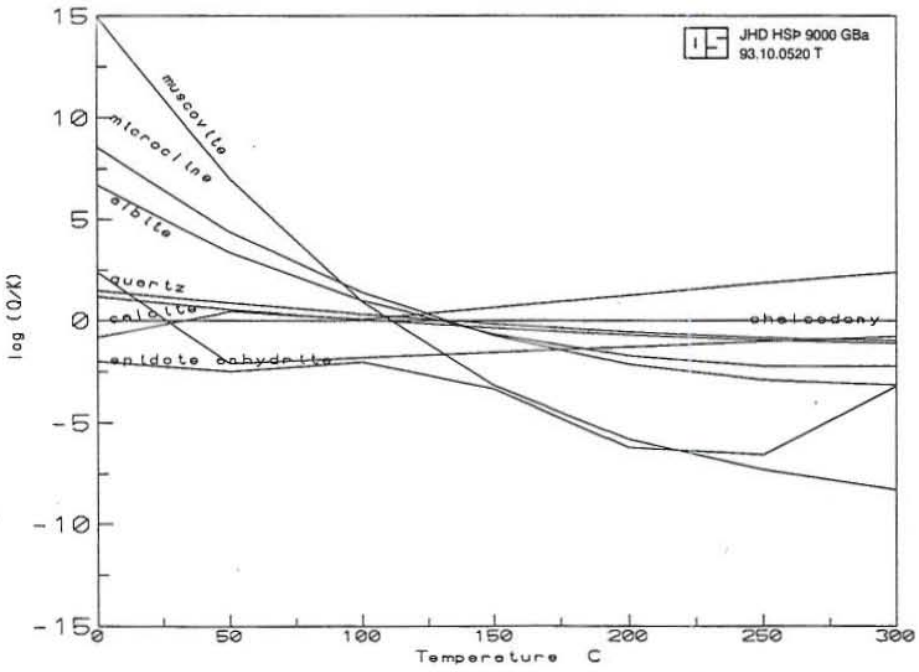

FIGURE 8: The saturation state of some minerals in water from the Buranga area, sample No. 012

appropriate minerals.

Reed and Spycher (1984) have taken a somewhat different approach to geothermometry. Their approach does not rest on the assumption of predetermined mineral/solute equilibria or the use of empirically calibrated geothermometers. It involves evaluating the state of saturation of water at a specific composition with a large number of minerals as a function of temperature (Figures 7-9). If a group of minerals is close to equilibrium at one particular temperature, the conclusion is that the water has equilibrated with this group of minerals and the temperature represents the aquifer temperature. Mixed waters and waters which are not close to equilibrium with hydrothermal minerals, like surface waters, are characterized by lack of apparent equilibration for many minerals at a particular temperature. The method is, thus, useful in distinguishing waters which have come close to equilibrium with hydrothermal minerals from mixed waters and non equilibrated waters. The procedure in constructingdiagrams like those depicted in Figures 7-9 requires the use of an aqueous speciation programme like WATCH (Arnorsson et al., 1982).

Aqueous speciation needs to be calculated at several predetermined temperatures to obtain a log (Q_i/K_i)-temperature relationship for each mineral for water composition under consideration.

Q_i is the reaction quotient and K_i is the equilibrium constant for mineral *i*. For example for albite we have

$$NaAlSi_3O_8 + 8H_2O = Na^+ + Al(OH)_4^- + 3H_4SiO_4^\circ \quad (11)$$

Assuming that albite is pure and the aqueous solution is very dilute, the activities of $NaAlSi_3O_8$ and H_2O can be taken to be equal to unity. Thus:

$$a_{Na} \cdot a_{Al(OH)_4} \cdot a^3_{H_4SiO_4} = Q_{ab} \quad (12)$$

where a_i indicates the activity of the ith species. The respective activities are computed by the programme to give a value of Q_{ab}. The solubility constant (K_{ab}) according to Equation 11 above is derived from chemical thermodynamic data.

Figures 7, 8 and 9 show the saturation states of hot spring waters from Katwe-Kikorongo, Buranga and Kibiro geothermal areas. There is apparent equilibration for most of the selected minerals at a temperature range of 120-130°C for the Katwe-Kikorongo and Buranga areas, and 140-150°C for the Kibiro area. This suggests that these minerals are in equilibrium with the fluid at these temperatures.

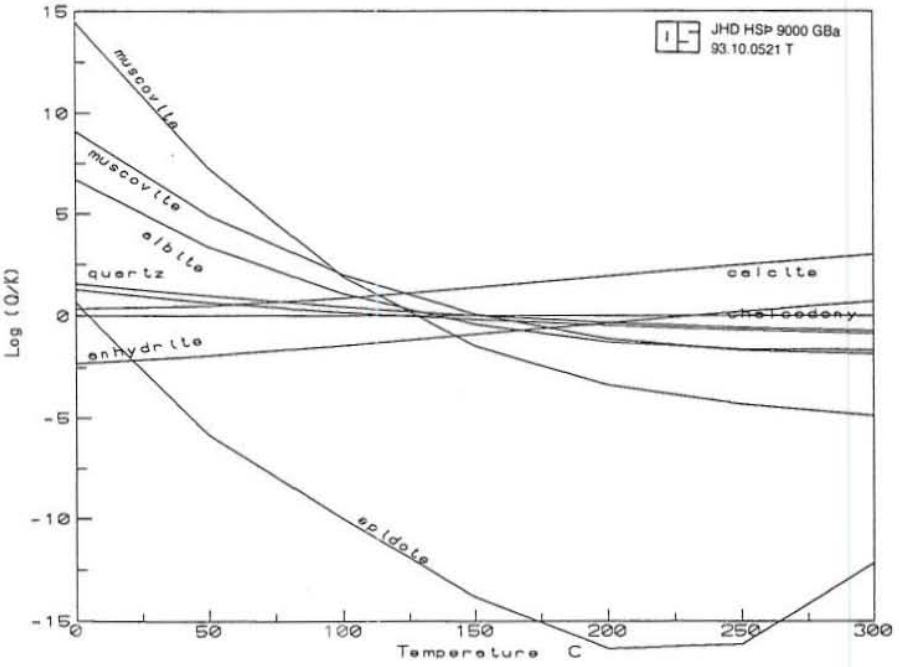

FIGURE 9: The saturation state of some minerals in water from the Kibiro area, sample No. 022

4.5 Evidence for mixing

Water formed by mixing of geothermal water and cold ground- or surface water possesses many chemical characteristics which serve to distinguish it from unmixed geothermal water. The reason is that the chemistry of geothermal waters is characterized by equilibrium between the chemical constituents in the water and alteration minerals, whereas the composition of cold waters appears to be determined mostly by the kinetics of the leaching process. The mixed waters tend to acquire characteristics which may be said to be intermediate between those just mentioned. It must, however, be realized that the residence time in the bedrock after mixing and the

temperature and salinity of the mixed water influence the final chemical composition of spring discharges. Strong conductive cooling of geothermal waters in the upflow zones and subsequent reaction with the rock may produce composition affinities similar to those obtained by leaching subsequent to mixing. Since geothermal waters often, but not always, contain much more dissolved solids than cold ground- and surface waters, the mixing process has often been referred to as dilution.

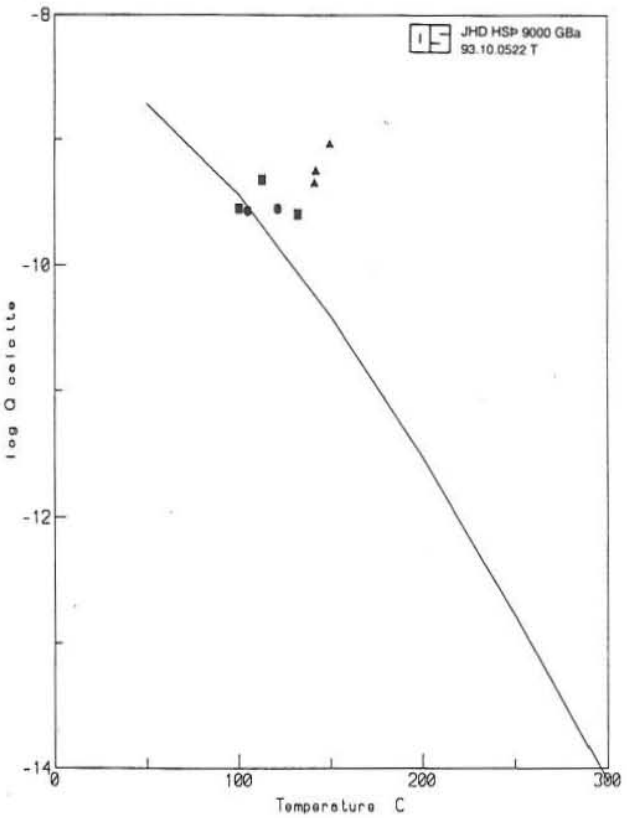

FIGURE 10: The state of calcite saturation at depth in the thermal waters from Katwe-Kikorongo (circles), Buranga (squares) and Kibiro (triangles); calcite saturation curve from data by Arnorsson et al. (1982)

The main chemical characteristics of mixed waters which serve to distinguish them from equilibrated geothermal waters, include relatively high concentrations of silica in relation to discharge temperature, low pH relative to water salinity and high total carbonate, at least if the mixing has prevented boiling and the temperature of the hot water component exceeds about 200°C. Further, like cold waters, mixed waters tend to be calcite undersaturated compared to geothermal water.

Figure 10 shows the state of calcite saturation at depth for waters from the Katwe-Kikorongo, Buranga and Kibiro geothermal areas. The data points for Katwe-Kikorongo and Buranga areas plot close to the equilibrium curve, which is based on data tabulated by Arnorsson et al. (1982), while those for Kibiro plot above the curve. This shows that the waters from Katwe and Buranga are close to saturation while the Kibiro waters are supersaturated with respect to calcium carbonate. The waters from Kibiro have high calcium and magnesium concentrations, probably due to mixing of the geothermal fluid with cold ground water.

Chloride and boron levels in cold water are low but high in geothermal water and, as these constituents are not considered to be incorporated in secondary minerals, mixing involves simple lowering of concentrations without affecting the Cl/B ratio. If mixing of geothermal water and cold water is responsible for variable chloride concentrations, it is to be expected that the intersection at 0 ppm boron of a line through the data points is in the range of 10 ppm chloride, as cold water contains chloride in that range and less than 0.01 ppm boron. Figure 11 shows the chloride-boron relationship for the waters from Katwe-Kikorongo, Buranga and Kibiro areas. In all cases there is a good linear relationship. Thus the chloride-boron relationships of the waters from these fields are taken to present a strong evidence for mixing.

Similarly linear relationships between silica and chloride, and sulphate and chloride could also give evidence for mixing. The waters from Katwe-Kikorongo show a close to linear relation between chloride and silica while the waters from Buranga and Kibiro show no relation at all (Figure 12).

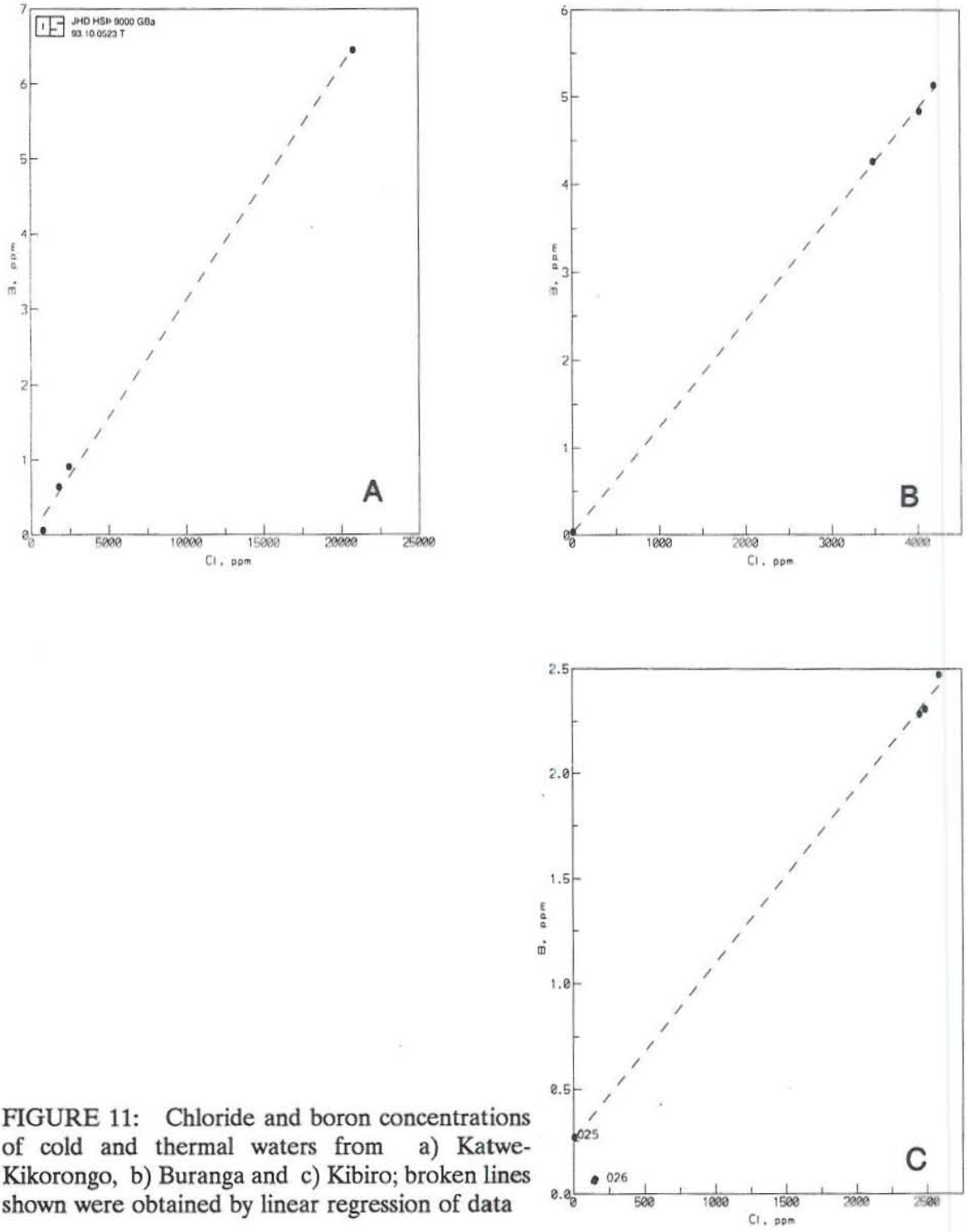

FIGURE 11: Chloride and boron concentrations of cold and thermal waters from a) Katwe-Kikorongo, b) Buranga and c) Kibiro; broken lines shown were obtained by linear regression of data

Sulphate concentrations show a good relation with chloride in waters from Katwe-Kikorongo and Buranga but no such relationship is observed for the Kibiro waters (Figure 13). The sulphate concentration of the waters from Katwe-Kikorongo and Buranga is generally higher than that of waters from Kibiro area. All waters in the three areas are undersaturated at depth with respect to anhydrite (Figure 14).

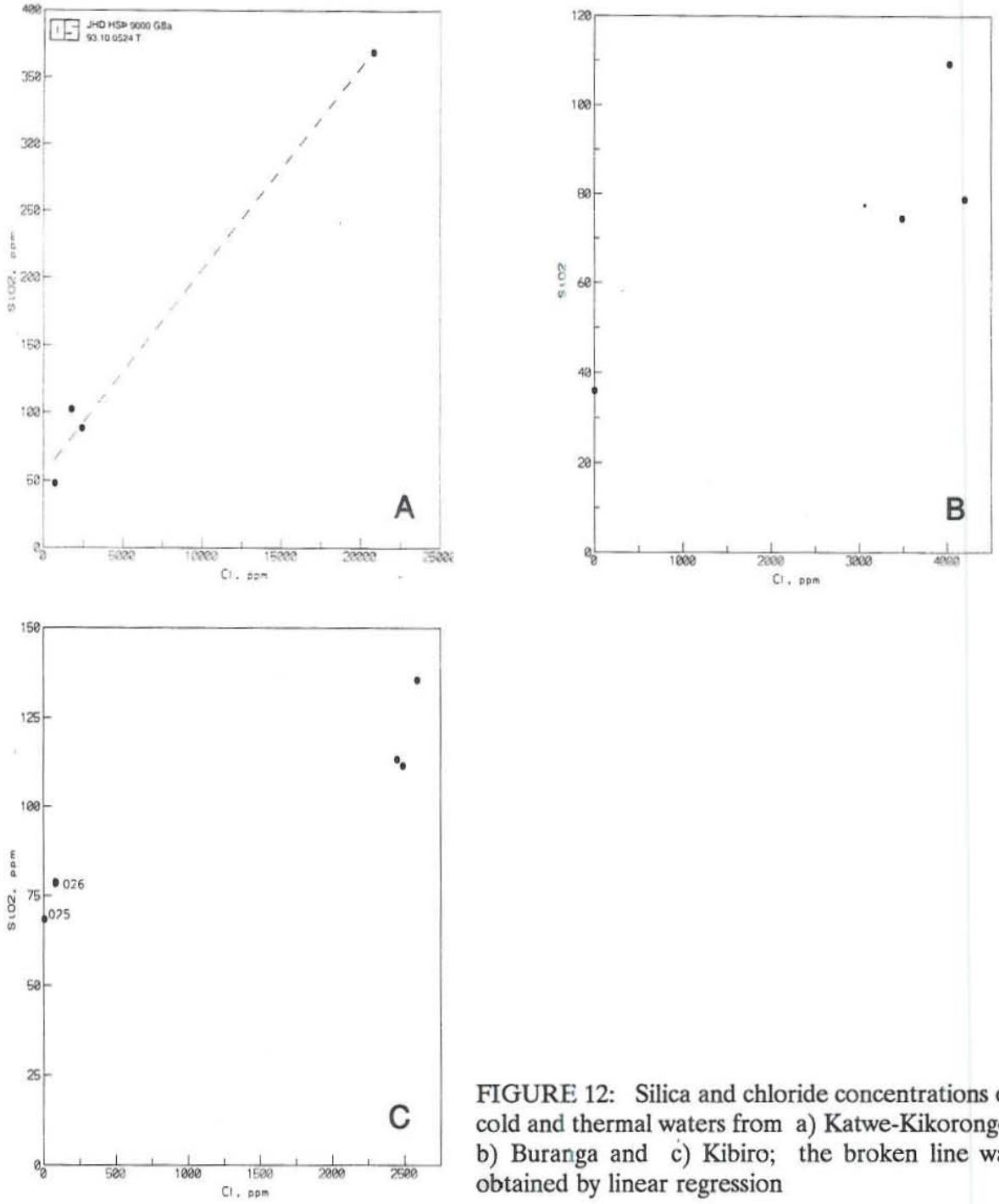

FIGURE 12: Silica and chloride concentrations of cold and thermal waters from a) Katwe-Kikorongo, b) Buranga and c) Kibiro; the broken line was obtained by linear regression

The lack of chloride-sulphate relationship for the Kibiro waters cannot, therefore, be explained by the control of anhydrite solubility upon sulphate mobility. It may be that redox equilibrium involving hydrogen sulphide and pH is the controlling factor:

$$H_2S + 4H_2O = SO_4^{2-} + 2H^+ \qquad (13)$$

It is important to note that two cold water samples, 025 and 026 are presented for Kibiro geothermal area (Figures 11, 12 and 13). It is not clear which of the two is probably mixing with the thermal water. They both give a good linear chloride-boron relationship and no silica-chloride

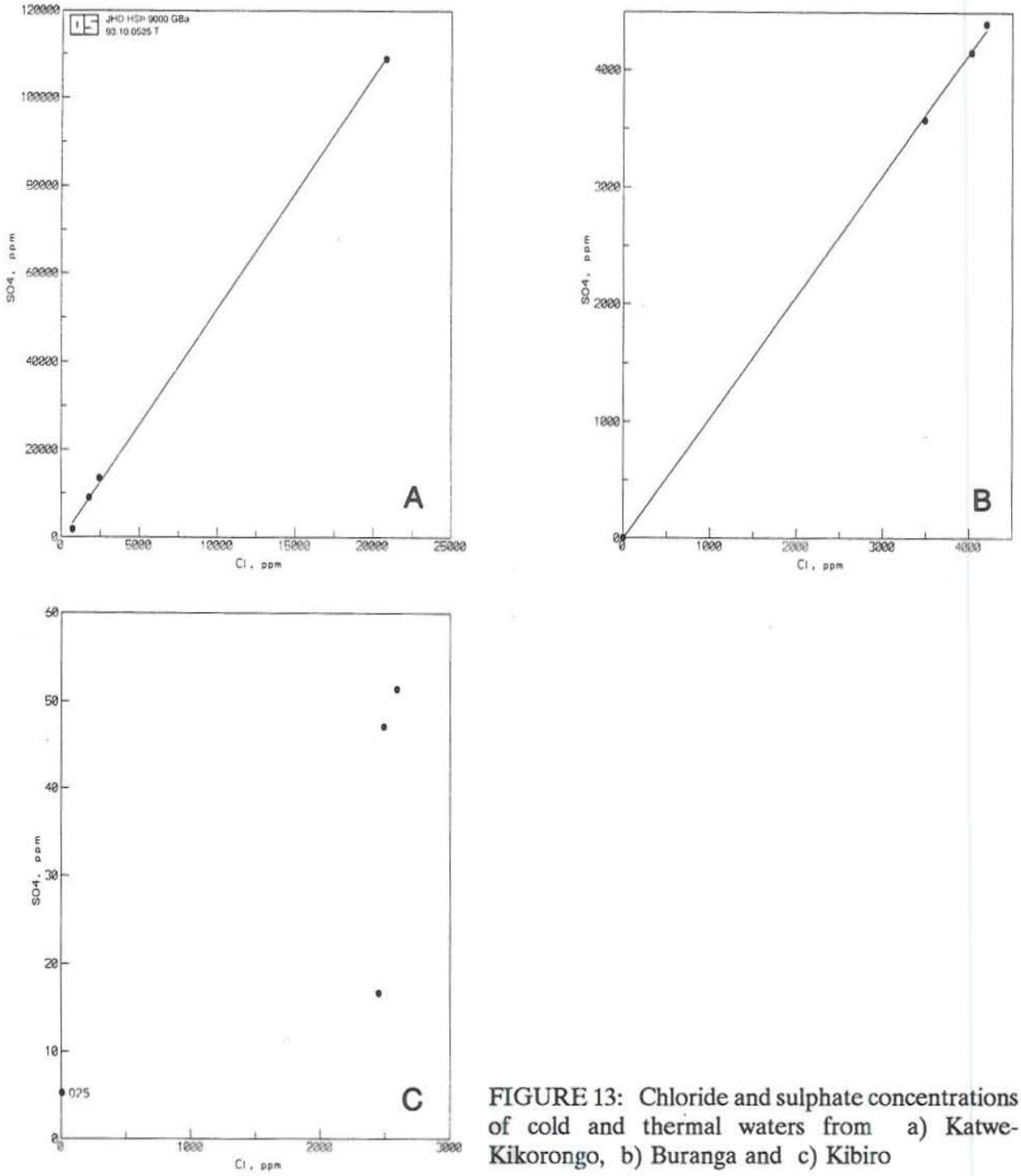

FIGURE 13: Chloride and sulphate concentrations of cold and thermal waters from a) Katwe-Kikorongo, b) Buranga and c) Kibiro

relationship with the thermal samples. The chloride-sulphate relation between the two cold water samples and thermal samples gives a negative trend for sample No. 026. Its sulphate concentration is so much higher than that of the corresponding thermal samples that it can not plot on the same scale and hence could not be considered as a mixing water. The analytical results of the two cold-water samples and the corresponding thermal samples are presented in Table 5. Therefore, sample No. 025 with a much lower sulphate concentration than the thermal samples was considered to be the most probable mixing water.

4.6 Silica solubility in hydrothermal solutions

The solubility of silica in hydrothermal solutions has been determined experimentally as a function of temperature at the vapour pressure of the solution. Pressure and added salts have little effect on the solubility of quartz and amorphous silica below about 300°C. Above 300°C, both pressure and added salts are very important. This information allows the dissolved concentration in a hydrothermal solution to be used as a chemical geothermometer. When using a silica geothermometer an assumption must be made about the particular silica mineral that is controlling the dissolved silica concentrations, and corrections may be required for the effects of decompressional boiling (adiabatic cooling). Also, below 340°C the solubility of amorphous silica decreases drastically as temperature decreases, so silica may precipitate from solution as a result of conductive or adiabatic cooling, before reaching the surface, causing low predicted reservoir temperatures. The solubility of quartz in water and coexisting steam at the vapour pressure of the solution up to the critical point for a very dilute solution is shown in Figure 15.

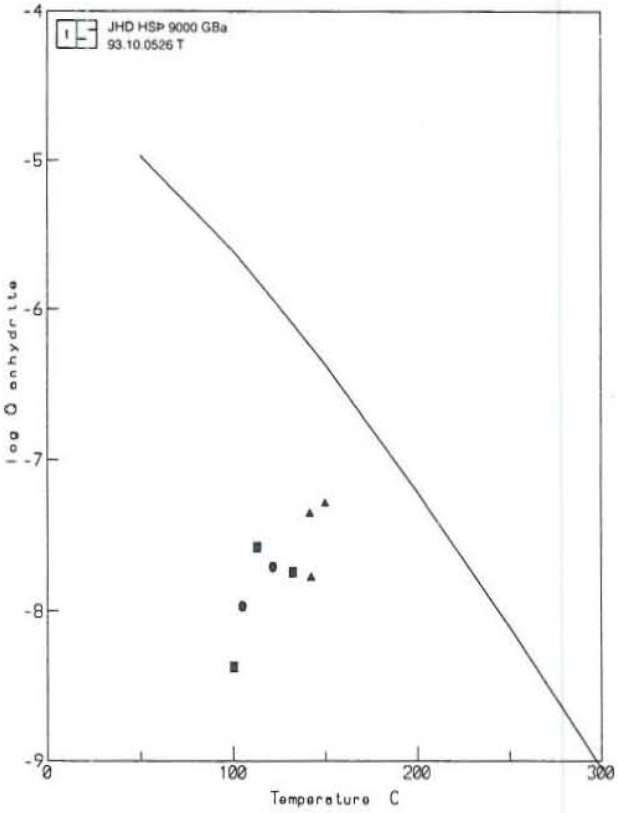

FIGURE 14: The state of anhydrite saturation at depth in the thermal waters from Katwe-Kikorongo (circles), Buranga (squares), Kibiro (triangles); quartz equilibrium curves as reference

4.7 The silica-enthalpy mixing model

The silica-enthalpy mixing model proposed by Fournier (1977) may be used as an aid to evaluate subsurface temperatures. It is based on the solubility of silica as described in the previous section. In this model, the dissolved silica concentration of a mixed water and a silica-enthalpy diagram may be used to determine the temperature of the hot-water component (Figure 16). A straight line drawn from a point representing a non-thermal component of the mixed water (point A) through a mixed-water warm spring (point B) to the intersection with the quartz solubility curve gives the initial silica concentration and enthalpy of the hot water component (point C). The original temperature of the hot water component is then obtained from steam tables (Keenan et al., 1969).

In this procedure it is assumed that any steam that forms adiabatically does not separate from the residual liquid water before mixing with the cold water component. In the case where steam is lost before mixing takes place, for instance at atmospheric pressure, a horizontal line drawn from point D to the intersection with the maximum steam loss curve gives the initial enthalpy of the hot water component (point E). The initial dissolved silica is shown by point F. Therefore, the assumption of mixing after maximum steam loss gives minimum temperatures, while the assumption of mixing without steam loss gives maximum temperatures.

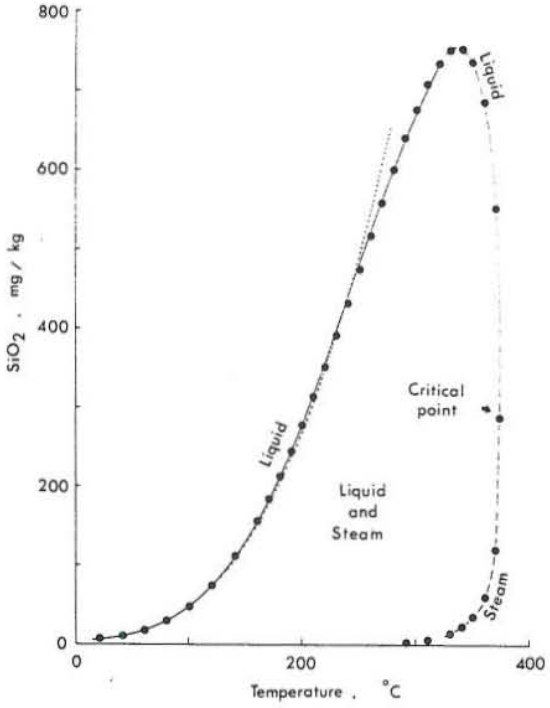

FIGURE 15: The solubility of quartz in water at the vapour pressure of the solution (Fournier and Potter, 1982)

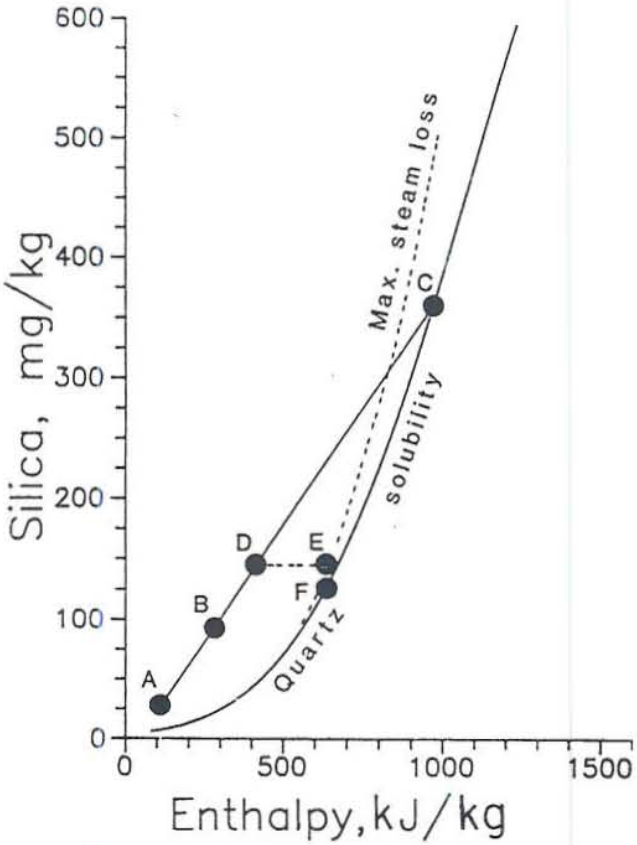

FIGURE 16: Silica-enthalpy diagram illustrating use in calculating silica mixing model temperatures

Figures 17, 18 and 19 show the silica-enthalpy graphs for the Katwe-Kikorongo, Buranga and Kibiro areas, respectively, and the results are summarized in Table 8. The diagrams show that the thermal waters of the Buranga and Katwe-Kikorongo areas, leaving out sample number 018, are probably mixing with little boiling while those for the Kibiro area are probably boiling and mixing.

4.8 The silica-carbonate mixing model

Arnorsson et al. (1983b) found that the concentrations of carbon dioxide in waters in geothermal reservoirs were only dependent on the temperatures of these waters. They concluded that this was the result of overall solute/mineral equilibration in these reservoirs. At a

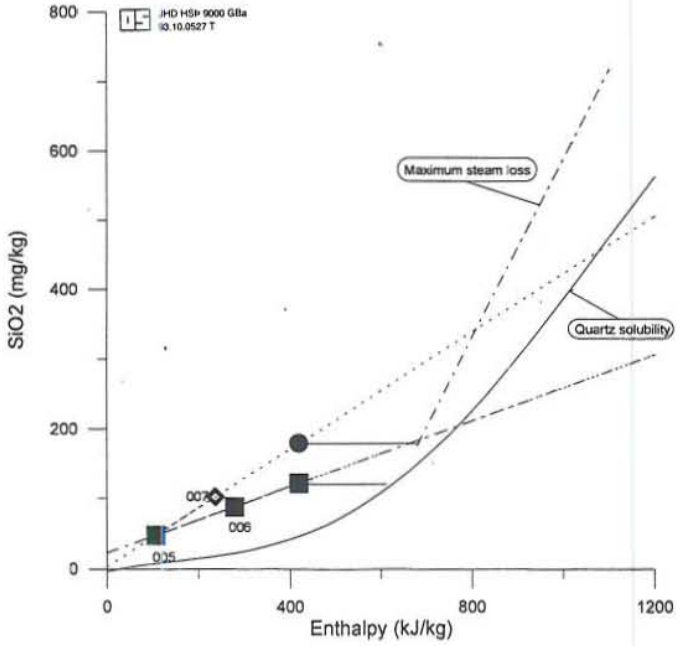

FIGURE 17: The silica-enthalpy graph for waters from the Katwe-Kikorongo area

temperature above about 200°C, almost all the dissolved total carbonate is in the form of carbon dioxide, so it is a satisfactory approximation to take analyzed carbonate to represent carbon dioxide. It is well known that silica levels in high temperature waters are determined by quartz solubility. It follows, therefore, that it is a satisfactory approximation to assume a fixed relation between silica and total carbonate in high temperature geothermal reservoir waters. Boiling of such waters will lead to a drastic reduction in its carbonate content but mixing without boiling will, on the other hand produce waters with high carbonate/silica ratios relative to the equilibrated waters, due to the curvature of the silica-carbonate relationship (Figure 20).

This model gives a hot water component temperature of 210°C for Kibiro area which was obtained by extrapolating a line through the data points for mixed and undegassed warm waters and determination of the point of intersection with the silica-carbonate curve for equilibrated waters and deriving the corresponding temperature from the quartz geothermometer. The silica-carbonate mixing model could not be applied to Katwe-Kikorongo and Buranga areas because of the high carbonate content of the waters in relation to silica. The working range of this model is 50-250°C, with a maximum silica concentration of 460 mg/kg and maximum total carbonate of 1100 mg/kg. The total carbonate concentration of the waters from the two areas as presented in Table 5 is outside the operation range of this model.

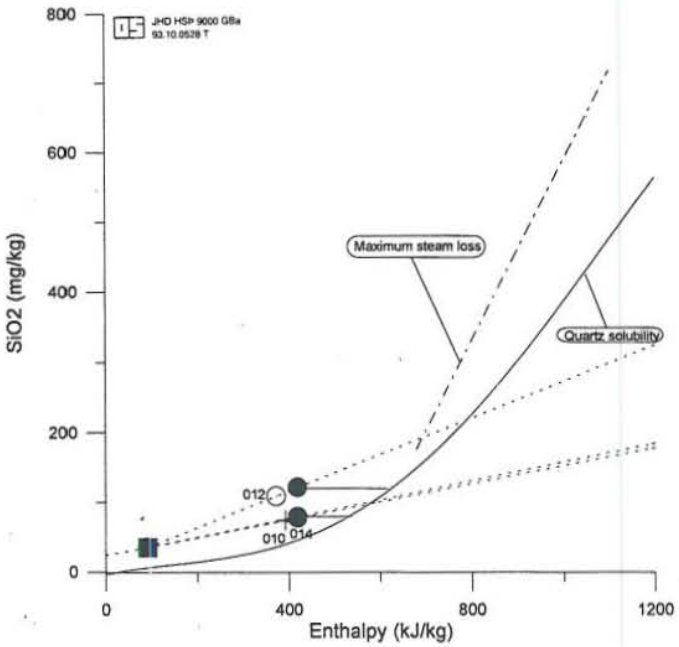

FIGURE 18: The silica-enthalpy graph for waters from the Buranga area

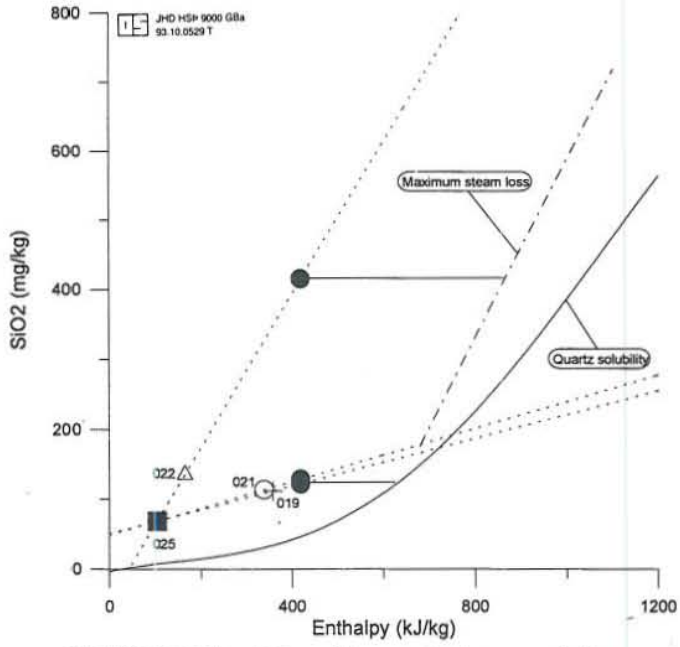

FIGURE 19: The silica-enthalpy graph for waters from the Kibiro area

TABLE 8: Results of the silica-enthalpy mixing model (Fournier 1977)

Area	Sample no.	Temperature with no steam loss before mixing (°C)	Temperature with maximum steam loss before mixing (°C)
Katwe-Kikorongo	007	250	160
	006	180	about 150
Buranga	012	190	about 150
	010 and 014	140	-
Kibiro	022	>300	205
	019 and 021	175	about 150

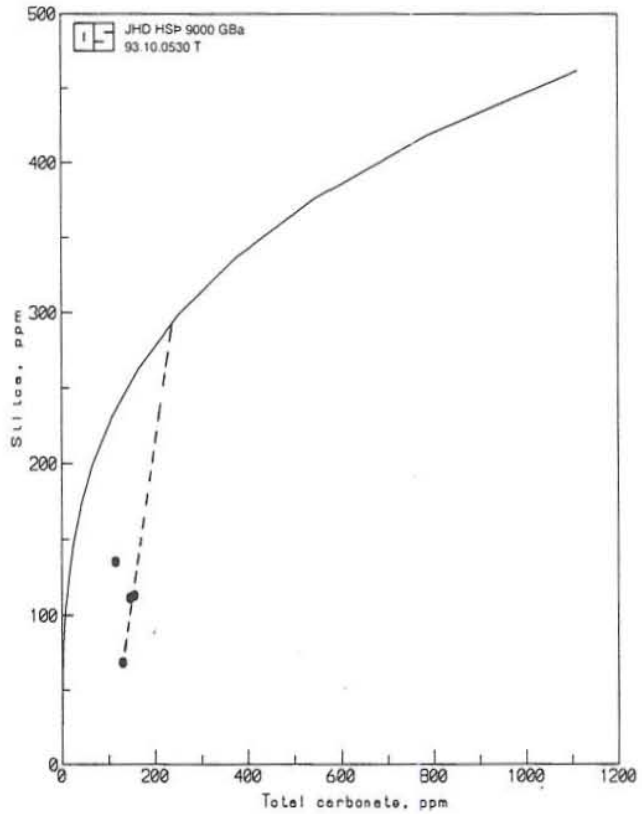

FIGURE 20: A plot of silica vs. total carbonate (silica-carbonate mixing model) for cold and thermal waters from Kibiro

5. DISCUSSION

The distribution of aqueous speciation calculated using the WATCH programme results in a good ionic balance between cations and anions with a percentage difference less than ±1.0 for all the geothermal samples from the three areas except sample number 018 which gives an ionic balance with a percentage difference of +8.94. The results from the calculation of aqueous speciation show sample number 018 not to be a true geothermal sample. This sample is from a hot spring which emerges from the bottom of a lake and the hot spring water is likely to have mixed with the lake water during sampling. Therefore, the aqueous speciation of sample number 018 could not be used in calculating geothermometer and mixing model temperatures. However, its analytical results were used in evaluation of the equilibrium state of the waters using triangular diagrams. The results from these diagrams show sample number 018 to be related to samples number 006 and 007 from the same area.

The initial assessment of the geothermal potential of the areas was done using triangular diagrams (Giggenbach, 1988). The Na-K-Mg diagram (Figure 5) shows the data points for Katwe-Kikorongo and Buranga thermal waters to be close to equilibrium but generally above the equilibrium line. This is probably due to loss of magnesium in the upflow zone as magnesium carbonate because of the high carbonate concentration of these waters. This does not rule out the possibility of mixing of the thermal and cold water in these areas. The data points for the Kibiro thermal waters plot in the area of partially equilibrated (including mixed) waters but close to the boundary with immature waters. This is most likely due to mixing with cold ground water. The Na/K and K/Mg geothermometer temperatures derived directly from this diagram tend to be high because it uses the analytical concentrations and not the activities which should be used in case of waters with high salinity. Therefore, these geothermometer temperatures were not used in prediction of subsurface temperatures. The Cl-SO_4-HCO_3 triangular diagram (Figure 6) shows the Kibiro thermal waters to be chloride-mature waters while those from Katwe-Kikorongo are sulphate-volcanic-steam heated waters. The Buranga thermal waters are chloride-sulphate volcanic waters. Therefore, the Kibiro waters should be suitable for the application of geoindicators.

From the geothermometry results (Table 7), the quartz and K/Mg geothermometers generally give lower results than the Na/K geothermometer probably due to quick re-equilibration with cooling in the upflow zone. The K/Mg geothermometer gives higher results than the Na/K geothermometer for Katwe-Kikorongo and Buranga areas probably due to loss of magnesium as magnesium carbonate because of the high carbonate content of the waters. In the Buranga area the quartz geothermometer gives higher results than the Na/K geothermometer probably due to loss of potassium from solution during cooling in the upflow zone. Potassium appears to be lost from solution, perhaps by precipitation of K-feldspar, but absorption into clays is also possible. In the latter case base exchange reactions involving clay rather than the feldspar may control the Na/K ratio. Reactions involving Na and K appear to proceed very slowly while those involving Mg appear to proceed relatively quickly.

In this regard, the salinity of the solution is an important factor because a given amount of a reaction of highly saline fluid with wall rock during upflow will have little effect on the ratios between the major cations in the solution. On the other hand, the same amount of reaction of a dilute solution with wall rock may drastically change the cation ratios. In highly saline solutions like these the Na/K ratio is considered to give more reliable results. There is a good agreement between Na/K, H_2S and H_2CO_3 geothermometers for the Kibiro area. This shows that H_2S and H_2CO_3 are in equilibrium with the fluid. The H_2CO_3 geothermometer could not be applied to the Katwe-Kikorongo and Buranga areas because of the high total carbonate which is likely not

to be in equilibrium with the fluid. The CaH geothermometer results can be explained in the same way as for the K/Mg geothermometer since the concentration of magnesium and calcium is controlled by the same factors.

The interpretation of chemical analyses of hot spring waters with respect to predicting underground temperatures should integrate as many parameters as possible into a single model rather than consider individual geothermometers and mixing models in isolation. In the present study use was made of almost all the components represented in Table 5. The following relationships provided enough evidence for mixing of thermal and cold water in all the three areas. The calcite saturation state at depth (Figure 10) shows that the thermal waters of Katwe-Kikorongo and Buranga are close to saturation while those for Kibiro are supersaturated. The concentration of calcium is very high like that of magnesium probably due to mixing with cold water whose magnesium and calcium concentrations are high. The chloride-boron relationship for the waters from the three areas is linear and this presents a strong evidence for mixing. The waters from Katwe-Kikorongo show a close to linear relationship between chloride and silica while the waters from Buranga and Kibiro show no relationship at all. Sulphate concentrations show a good relation with chloride in waters from Katwe-Kikorongo and Buranga areas but not for Kibiro. The waters from Katwe-Kikorongo and Buranga are generally high in sulphate. All thermal waters in the three areas are undersaturated at depth with respect to anhydrite (Figure 14).

Lack of a chloride-sulphate relationship for the Kibiro waters cannot, therefore, be explained by the control of anhydrite solubility upon sulphate mobility. It may be that a redox equilibrium involving hydrogen sulphide and pH is the controlling factor (Equation 13). Two cold water samples are considered for the Kibiro area (Figures 11, 12 and 13). It is not clear which one is the mixing cold water, although, sample No. 025 was assumed to be the most probable mixing water because of its low sulphate concentration as compared to the thermal samples. This demonstrates that there are more types of ground water in the area than the one used and that the situation as regards mixing may be more complicated than presented.

The results of the silica-enthalpy mixing model (Table 8) show that the thermal waters of the Katwe-Kikorongo and Buranga areas are probably mixing with little boiling while those for Kibiro are probably boiling and mixing. The silica-enthalpy mixing model gives minimum temperatures of 150-160°C for the Katwe-Kikorongo area, less than 150°C for the Buranga area and 150-205°C for the Kibiro area. The silica-carbonate mixing model gives a temperature of 210°C for the Kibiro area. This is in agreement with the silica-enthalpy mixing model temperature of 205°C and the Na/K, H_2S, H_2CO_3 geothermometer temperatures (Table 5). The silica-carbonate mixing model could not be applied to the Katwe-Kikorongo and Buranga areas because of the high carbonate content which is outside the operation range of the model.

6. CONCLUSIONS AND RECOMMENDATIONS

The present study has shown that the thermal waters of the Katwe-Kikorongo and Buranga areas are sulphate-volcanic-steam heated waters with high carbonate while those of the Kibiro area are chloride-mature waters. All observations for the Katwe-Kikorongo area give a temperature range of 105-250°C with an average of 158°C predicting subsurface temperatures of 150-160°C, but the results for a sample collected from an upflow at the bottom of Lake Kitagata remains unresolved. All observations for the Buranga area give a temperature range of 100-190°C with an average of 126°C predicting subsurface temperatures of 120-130°C. All observations for the Kibiro area give a temperature range of 140 to above 300°C with two groups of averages: the quartz and K/Mg geothermometers predict average subsurface temperatures of 150-160°C while the Na/K, H_2S, H_2CO_3 and mixing models predict subsurface temperatures of 200-210°C.

Finally, the author recommends that the source of sample number 018 should be re-examined in order to establish the more reliable subsurface temperatures for the Katwe-Kikorongo area. He also recommends that further investigations in these areas should continue.

ACKNOWLEDGEMENTS

I wish to acknowledge the United Nations Development Programme for giving me the opportunity to attend this course which will be very useful to me and to the Government of Uganda. Special thanks to Dr. Halldor Armannsson for his guidance and advice in writing this report. Thanks to Dr. Ingvar Fridleifsson and Mr. Ludvik Georgsson for their guidance through the course. Many thanks to the staff of Orkustofnun and the UNU fellows for their support during the course. Many thanks to Mr. Kristjan Hrafn Sigurdsson for his assistance in the analysis of water samples. The Government of Uganda is acknowledged for allowing me to undertake this training.

REFERENCES

Arad, A., and Morton, W.H., 1969: Mineral springs and saline lakes of Western rift valley, Uganda. Geochim. Cosmochim. Acta, 33, 1169-1181.

Arnorsson, S., and Bjarnason, J.O., 1993: Icelandic Water Chemistry Group presents the chemical speciation programme WATCH. Science Institute, University of Iceland, Orkustofnun, Reykjavik, 7 pp.

Arnorsson, S., Gronvold, H., and Sigurdsson, S., 1978: Aquifer chemistry of four high temperature geothermal systems in Iceland. Geochim. Cosmochim. Acta, 42, 523-536.

Arnorsson, S., Sigurdsson, S., and Svavarsson, H., 1982: The chemistry of geothermal waters in Iceland. I. Calculation of aqueous speciation from 0° to 370°C. Geochim. Cosmochim. Acta, 46, 1513-1532.

Arnorsson, S., Gunnlaugsson, E., and Svavarsson, H., 1983a: The chemistry of geothermal waters in Iceland II. Mineral equilibria and independent variables controlling water compositions. Geochim. Cosmochim. Acta, 47, 547-566.

Arnorsson, S., Gunnlaugsson, E., and Svavarsson, H., 1983b: The chemistry of geothermal waters in Iceland. III. Chemical geothermometry in geothermal investigations. Geochim. Cosmochim. Acta, 47, 567-577.

Connah, G., Kamuhangire, E., and Piper, A., 1990. Salt production at Kibiro. Azania, 27-39.

Dixon, C.G., and Morton, W.H., 1967: Thermal and mineral springs in Uganda. UGMS, unpubl. report no. WHM/5-CGD/17.

Dixon, C.G., and Morton, W.H., 1970: Thermal and mineral springs in Uganda. Geothermics, sp.is. 2, 2, 1035-1038.

Ellis, A.J., and Mahon, W.A.J., 1977: Chemistry and geothermal systems. Academic press, New York, 392 pp.

Fournier, R.O., 1977: Chemical geothermometers and mixing models for geothermal systems. Geothermics, 5, 41-50.

Fournier, R.O., and Potter, R.W. II., 1982: An equation correlating the solubility of quartz in water from 25°C to 900°C at pressures up to 10,000 bars. Geochim. Cosmochim. Acta, 46, 1969-1974.

Giggenbach, W.F., 1981: Geothermal mineral equilibria, Geochim. Cosmochim. Acta, 45, 393-410.

Giggenbach, W.F., 1984: Mass transfer in hydrothermal alteration systems. Geochim. Cosmochim. Acta, 48, 2693-2711.

Giggenbach, W.F., 1988: Geothermal solute equilibria. Derivation of Na-K-Mg-Ca geoindicators. Geochim. Cosmochim. Acta, 52, 2749-2765.

Gislason, G., Ngobi, G., Isabirye, E., and Tumwebaze, S., 1993: An inventory of three geothermal areas in W and SW Uganda. UNDP/GSMD Report.

Gislason, S.R., and Eugster, H.P., 1987a: Meteoric water-basalt interactions: I. A laboratory study. Geochim. Cosmochim. Acta, 51, 2827-2840.

Gislason, S.R., and Eugster, H.P., 1987b: Meteoric water-basalt interactions: II. A field study in NE Iceland. Geochim. Cosmochim. Acta, 51, 2841-2855.

Gunnlaugsson, E., 1977: The origin and distribution of sulphur in fresh and geothermally altered rocks in Iceland. Unpubl. PhD. thesis, Leeds Univ., 192 pp.

Keenan, J.H., Keyes, F.G., Hill, P.G., and Moore, J.G., 1969: Steam Tables. John Wiley & Sons, New York, 162 pp.

Maasha-Ntungwa, 1974: Electrical resistivity and micro earthquake surveys of Buranga, L. Kitagata and Kitagata geothermal anomalies, Western Uganda. UGSM, unpubl. report.

Musisi, J., 1991: The neogene geology of the Lake George-Edward basin, Uganda. Unpubl. PhD. thesis, Vrije Universiteit Brussel, 299 pp.

Reed, M., and Spycher, N., 1984: Calculation of pH and mineral equilibria in hydrothermal waters with application to geothermometry and studies of boiling and dilution. Geochim. Cosmochim. Acta, 48, 1479-1492.

Scott-Elliot, G.F., and Gregory, J.W., 1895: The geology of Mount Ruwenzori and some adjoining regions of Equatorial Africa. Quart. J. Geol. Soc., 51, 669-680.

Sharma, D.V., 1970: Report on the possibility of occurrence and use of geothermal energy in Uganda. UGSM, report no. DVS/1.

Sharma, D.V., 1971: Report on the preliminary survey of thermal anomalies of western Uganda for the possible development of geothermal energy. UGSM, report no. DVS/3, 22 pp.

Sharma, D.V., 1973: Interpretation of the chemical results from thermal waters of Kitagata, L. Kitagata, Buranga and Kibiro. UGSM, report no. DVS/12, 12 pp.

Stanley, H.M., 1890: In Darkest Africa (2 vol.). C. Scribner's Sons, New York, vol. 1, 547 pp and 73 illus. & maps; vol. 2, 540 pp and 72 illus. & maps.

Stefansson, V., 1987: Geothermal resources of Uganda. Review of chemical data. United Nations, New York, 19 pp.

Wayland, E.J., 1935: Notes on thermal and mineral springs in Uganda. UGMS, Bull. 2., 44-54.

APPENDIX I: Geochemical sampling in geothermal areas

Figure 1 shows a sample field record card and the table below how to fill in part of it. In the laboratory a different record card is recommended in order to keep track of all chemical analyses. An outline of such a card is shown in Figure 2. Figure 3 shows the general setup and the apparatus used for collection of water and gas from a spring.

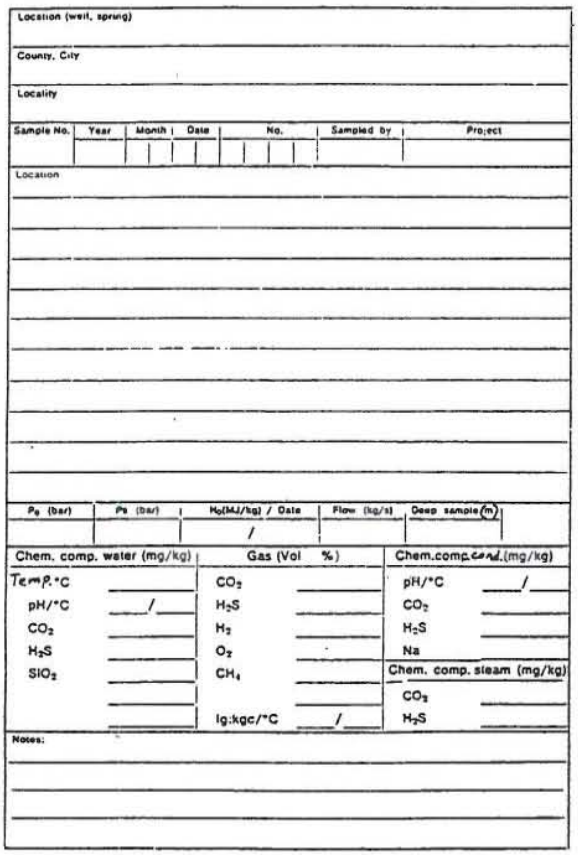

FIGURE 1: A sample field record card

Year	Month	Day	Sample no.
93	02	28	006

RESULT OF CHEMICAL ANALYSIS OF GEOTHERMAL SAMPLE

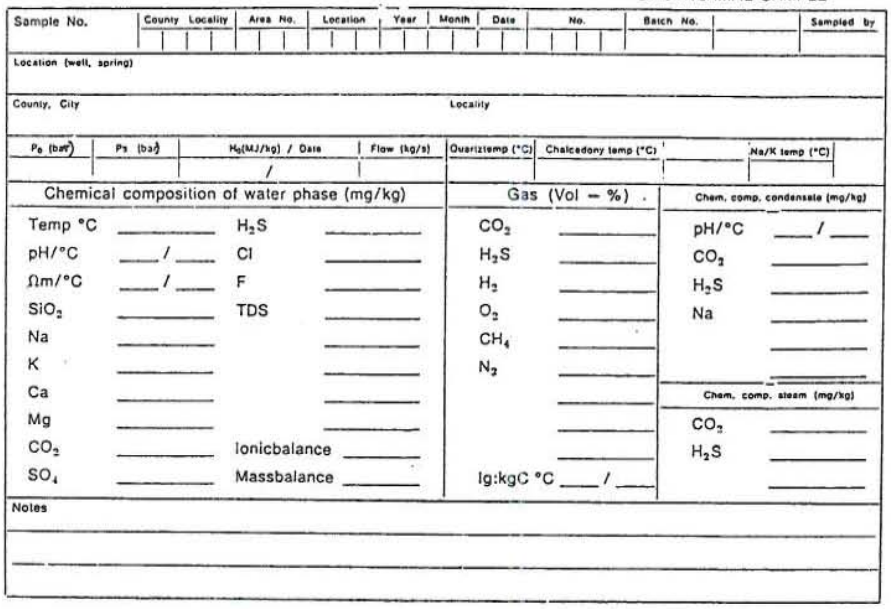

FIGURE 2: A laboratory card for chemical analyses

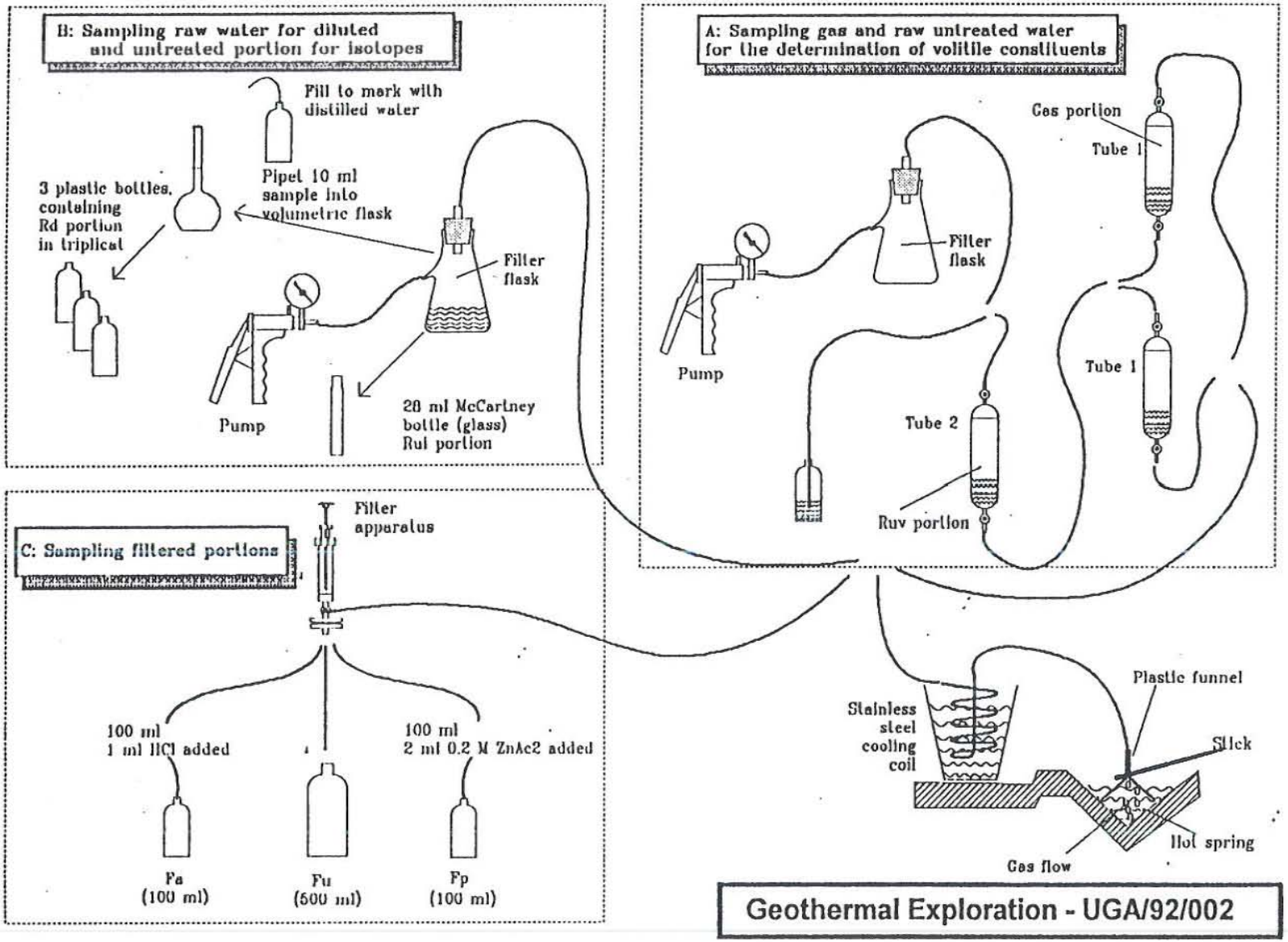

FIGURE 3: General setup and apparatus used for the collection of water and gas samples from a spring

Fa: Filtered, acidified, 100 ml sample + 1 ml, for cations; Fp: Filtered, precipitated, 100 ml sample + 2 ml Zn(Ac)2, for sulphate;
Fu: Filtered, untreated, for other anions; Rd: Raw, diluted, for silica

APPENDIX II: A printout of the sample output file of the WATCH programme

```
Icelandic Water Chemistry Group                                   Program WATCH, version 2.0 / 1993

GBB                          KIBIRO WATER CHEMISTRY

================================================================================================================

022              Kibiro


Water sample (mg/kg)          Steam sample

pH/deg.C          8.05/ 25.0  Gas (volume %)                Reference temperature    deg.C :  149.8  (Quartz)
CO2             115.00        CO2                 .00
H2S               .00         H2S                 .00      Sampling pressure     bar abs. :    1.0
NH3               .00         NH3                 .00      Discharge enthalpy       kJ/kg :  631.  (Calculated)
B                2.47         H2                  .00      Discharge                 kg/s :    .0
SiO2           135.50         O2                  .00      Steam fraction at collection   :  .0000
Na            1570.00         CH4                 .00
K              182.00         N2                  .00      Measured temperature     deg.C :   39.5
Mg               8.710
Ca              75.90         Liters gas per kg
F                4.910        condensate/deg.C   .00/  .0  Condensate (mg/kg)
Cl            2590.00                                      pH/deg.C          .00/  .0
SO4             51.40         Total steam (mg/kg)          CO2               .00
Al               .029         CO2                 .00      H2S               .00
Fe               .030         H2S                 .00      NH3               .00
TDS              .00          NH3                 .00      Na                .00

Ionic strength =  .07974
Ionic balance :  Cations (mol.eq.) =  .07722315    Anions (mol.eq.) =  .07684971    Difference (%) =  .48


Deep water components (mg/kg)                              Deep steam (mg/kg)       Gas pressures (bar-abs.)

B              2.47        CO2          115.00             CO2          .00         CO2        .360E-01
SiO2         135.50        H2S            .00              H2S          .00         H2S        .000E+00
Na          1570.00        NH3            .00              NH3          .00         NH3        .000E+00
K            182.00        H2             .00              H2           .00         H2         .000E+00
Mg             8.710       O2             .00              O2           .00         O2         .000E+00
Ca            75.90        CH4            .00              CH4          .00         CH4        .000E+00
F              4.910       N2             .00              N2           .00         N2         .000E+00
Cl          2590.00                                                               H2O        .473E+01
SO4           51.40                                                               Total      .477E+01
Al             .0290
Fe             .0300
TDS            .00         Aquifer steam fraction =  .0000

Ionic strength =  .07772                                                  1000/T (Kelvin) =  2.36
Ionic balance :  Cations (mol.eq.) =  .07565197    Anions (mol.eq.) =  .07528892    Difference (%) =  .48

Oxidation potential (volts) :    Eh H2S= 99.999   Eh CH4= 99.999   Eh H2= 99.999   Eh NH3= 99.999

Chemical geothermometers (degrees C)
Quartz      149.8  (Fournier & Potter, GRC Bulletin, pp. 3-12, Nov. 1982)
Chalcedony  124.3  (Fournier, Geothermics, vol. 5, pp. 41-50, 1977)
Na/K        216.8  (Arnorsson et al., Geochim. Cosmochim. Acta, vol. 47, pp. 567-577, 1983)
```

022

Activity coefficients in deep water

H+	.783	KSO4-	.741	Fe++	.323	FeCl+	.720
OH-	.711	F-	.711	Fe+++	.118	Al+++	.118
H3SiO4-	.720	Cl-	.702	FeOH+	.735	AlOH++	.309
H2SiO4--	.309	Na+	.720	Fe(OH)3-	.735	Al(OH)2+	.741
H2BO3-	.693	K+	.702	Fe(OH)4--	.300	Al(OH)4-	.728
HCO3-	.720	Ca++	.323	Fe(OH)++	.300	AlSO4+	.728
CO3--	.288	Mg++	.365	Fe(OH)2+	.741	Al(SO4)2-	.728
HS-	.711	CaHCO3+	.749	Fe(OH)4-	.741	AlF++	.309
S--	.300	MgHCO3+	.720	FeSO4+	.735	AlF2+	.741
HSO4-	.728	CaOH+	.749	FeCl++	.300	AlF4-	.728
SO4--	.275	MgOH+	.755	FeCl2+	.735	AlF5--	.288
NaSO4-	.741	NH4+	.693	FeCl4-	.720	AlF6---	.061

Chemical species in deep water - ppm and log mole

Deep water pH is 7.432

H+	.00	-7.326	Mg++	7.44	-3.514	Fe(OH)3	.00	.000
OH-	1.49	-4.057	NaCl	65.13	-2.953	Fe(OH)4-	.00	.000
H4SiO4	198.41	-2.685	KCl	2.25	-4.521	FeCl+	.00	-7.385
H3SiO4-	12.41	-3.884	NaSO4-	6.63	-4.255	FeCl2	.00	-15.656
H2SiO4--	.01	-7.024	KSO4-	2.52	-4.729	FeCl++	.00	.000
NaH3SiO4	7.10	-4.221	CaSO4	5.78	-4.372	FeCl2+	.00	.000
H3BO3	13.49	-3.661	MgSO4	4.30	-4.447	FeCl3	.00	.000
H2BO3-	.63	-4.986	CaCO3	4.31	-4.365	FeCl4-	.00	.000
H2CO3	16.51	-3.575	MgCO3	.14	-5.789	FeSO4	.00	-8.877
HCO3-	124.06	-2.692	CaHCO3+	25.76	-3.594	FeSO4+	.00	.000
CO3--	.39	-5.190	MgHCO3+	.67	-5.107	Al+++	.00	-20.730
H2S	.00	.000	CaOH+	.17	-5.519	AlOH++	.00	-14.810
HS-	.00	.000	MgOH+	.30	-5.140	Al(OH)2+	.00	-9.544
S--	.00	.000	NH4OH	.00	.000	Al(OH)3	.04	-6.329
H2SO4	.00	-16.552	NH4+	.00	.000	Al(OH)4-	.12	-6.218
HSO4-	.00	-7.557	Fe++	.01	-7.014	AlSO4+	.00	-21.487
SO4--	36.75	-3.417	Fe+++	.00	.000	Al(SO4)2-	.00	-23.148
HF	.00	-6.836	FeOH+	.02	-6.479	AlF++	.00	-16.860
F-	4.91	-3.588	Fe(OH)2	.01	-7.190	AlF2+	.00	-14.491
Cl-	2549.42	-1.143	Fe(OH)3-	.00	-8.824	AlF3	.00	-13.814
Na+	1541.71	-1.174	Fe(OH)4--	.00	-13.430	AlF4-	.00	-14.767
K+	180.09	-2.337	Fe(OH)++	.00	.000	AlF5--	.00	-16.709
Ca++	62.14	-2.810	Fe(OH)2+	.00	.000	AlF6---	.00	-19.666

Log solubility products of minerals in deep water

	Theor.	Calc.		Theor.	Calc.		Theor.	Calc.
Adularia	-15.668	-16.652	Albite, low	-15.072	-15.479	Analcime	-12.171	-12.793
Anhydrite	-6.363	-7.278	Calcite	-10.395	-9.032	Chalcedony	-2.493	-2.685
Mg-Chlorite	-80.044	-73.671	Fluorite	-10.561	-10.772	Goethite	-2.678	99.999
Laumontite	-25.407	-26.255	Microcline	-16.737	-16.652	Magnetite	-25.805	99.999
Ca-Montmor.	-76.858	-97.407	K-Montmor.	-36.819	-49.543	Mg-Montmor.	-78.198	-98.059
Na-Montmor.	-36.965	-48.370	Muscovite	-18.997	-20.455	Prehnite	-35.829	-35.281
Pyrrhotite	-74.706	99.999	Pyrite	-111.608	99.999	Quartz	-2.685	-2.685
Wairakite	-23.902	-26.255	Wollastonite	9.473	8.878	Zoisite	-35.406	-37.183
Epidote	-39.793	99.999	Marcasite	-90.894	99.999	Talc	12.799	21.996
Chrysotile	20.085	27.366	Sil. amorph.	-1.987	-2.685			